Estudio teórico y experimental de la pirólisis de biomasa y residuos en lecho fluidizado

Devolatilization of biomass and waste in fluidized bed: experiments and single-particle fuel conversion modeling

Trabajo Fin de Master

Master en Tecnología Química y Ambiental

Susanna Nilsson

Noviembre 2009

RESUMEN EN ESPAÑOL

1. Introducción

La devolatilización es un proceso clave durante la gasificación y combustión de biomasas y residuos, ya que durante esta etapa, ente un 70 y un 90 % de la masa combustible es emitida en forma de volátiles. La masa restante se transforma en carbonizado. La cantidad de carbonizado que se produce es importante para conocer el tamaño de lecho que se requiere en un gasificador para conseguir una conversión de carbono determinada, mientras que el contenido de alquitranes es un factor limitante para la aplicación posterior del gas producido durante la gasificación.

Para modelar el comportamiento de gasificadores de biomasa y residuos se emplean en muchos casos modelos de devolatilizacion de una partícula de combustible. Estos modelos no suelen permitir predecir las producciones de volátiles y de carbonizado, ni la composición de los volátiles sino que estos parámetros se estiman a partir de resultados experimentales obtenidos en un laboratorio. Para que los datos experimentales sean útiles para modelos de lecho fluidizado es necesario que hayan sido obtenidos a velocidades de calentamiento altas y a temperaturas elevadas (750-900 ºC). La distribución de productos obtenida durante la devolatilización depende en gran medida de la naturaleza y composición del material de partida y por esta razón no es recomendable extrapolar datos experimentales obtenidos para un tipo de biomasa o residuo a otra sustancia bien distinta.

En este trabajo se han llevado a cabo experimentos en lecho fluidizado, a escala de laboratorio, con el fin de estudiar la devolatilización de madera y algunos residuos. Los experimentos han sido realizados a temperaturas comprendidas entre 750 y 900 ºC, que es un rango de temperaturas de gran interés para la gasificación de biomasas y de

residuos. Los residuos estudiados son: harinas cárnicas (HAC), compost de residuos sólidos urbanos y lodos de depuradora secos.

Los resultados más importantes obtenidos a partir de los experimentos son las producciones de carbonizado, sustancias condensables y gases ligeros, así como la composición de la fracción de gases ligeros y el tiempo necesario para completar la devolatilización. Las mediciones, durante los ensayos, de las concentraciones de los componentes ligeros en el gas de salida también han permitido modelar la conversión de pellets de madera y partículas de lodos secos de depuradora.

2. Procedimiento experimental

Los materials objeto del estudio se recibieron en formas muy diferentes, la madera en forma de pellets de 6 mm de diámetro, los lodos de depuradora secos en forma de partículas aproximadamente esféricas y de tamaños comprendidos entre 1 y 5 mm, aunque las partículas con tamaños entre 2 y 4 mm representan el 98 % en peso de los lodos. Las harinas cárnicas y el compost se recibieron en forma de polvo. A partir de los materiales en polvo se prepararon manualmente pellets de 10 mm de diámetro, ya que si se alimentaran al reactor en forma de polvo las velocidades en lecho provocarían el arrastre de estos materiales. Como material inerte en el lecho se empleó ofita, un silicato subvolcánico de tamaños de partícula de 0.5 – 1 mm y con una densidad de 2650 kg/m^3.

El aparato experimental empleado consta de un reactor de lecho fluidizado con un diámetro del lecho de 26.6 mm y diámetro del "freeboard" de 52 mm. El gas entra al reactor por la parte de abajo, a través de un plato distribuidor con 27 agujeros de 1 mm. El reactor está equipado con un horno con control de temperatura que permite mantener una temperatura constante en el lecho. La biomasa se alimenta al reactor de forma discontinua por medio de una tolva conectada a un tubo de acero inoxidable equipado con dos válvulas de bola. A la salida del reactor se encuentran una serie de elementos que tienen como objetivo limpiar el gas producto antes de emitirlo a la atmósfera. Estos elementos son: un borboteador con isopropanol, un borboteador con agua destilada, un filtro, un lecho con gel de sílice. El isopropanol y el filtro sirven para retener partículas y alquitranes, mientras que el agua sirve para retener el isopropanol. Al final de la línea se encuentra el analizador de gases que mide de forma continua las concentraciones molares de CO, CO_2, CH_4, H_2 y O_2 en los gases de salida.

Durante los ensayos de devolatilización el reactor se fluidiza con nitrógeno de calidad industrial y las velocidades superficiales empleadas son de 0.5 y 0.8 m/s que son velocidades que están por encima de la velocidad mínima de fluidización. Las producciones de CO, CO_2, CH_4 y H_2 se calculan como las cantidades totales de estas susntancias detectadas por el enalizador a lo largo del ensayo. El final de la devolatilización se detecta cuando las concentraciones de las sustancias medidas por el analizador son cero. En este momento se empieza a alimentar aire al reactor para quemar el residuo carbonoso que queda después de la pirólisis. La cantidad total de carbonizado se calcula como la masa total de carbono en forma de CO y CO_2 detectada por el analizador durante esta etapa. Durante la combustión del carbonizado no se detectan cantidades apreciables de CH_4, por lo que se asume que el carbonizado no contiene hidrógeno. La cantidad de condensables obtenidos durante la pirólisis no es medida sino que se calcula por diferencia y esto implica que no es posible comprobar si

se cierran los balances de materia. La fracción de condensables calculada no solo incluye la cantidad de alquitrán que se ha formado sino también las cantidades de otras sustancias, principalmente agua e hidrocarburos ligeros (excepto el CH_4). Datos encontrados en la literatura muestran que la cantidad de agua química formada durante la devolatilización de biomasa varía poco con la temperatura en el rango de temperaturas objeto de este estudio, por lo que se puede asumir que las variaciones en la producción de condensables con la temperatura son consecuencia principalmente de las variaciones en la producción de alquitranes.

Durante los ensayos se ha estudiado los efectos de diferentes parámetros sobre los resultados. Estos parámetros son: temperatura en el lecho, tamaño de partícula del combustible, velocidad de fluidización y la cantidad de combustible alimentada al reactor.

Para estudiar el proceso de devolatilización también se ha calculado la evolución con el tiempo de la conversión de la biomasa a partir de la cantidad de volátiles detectada por el analizador en cada momento:

$$x_{dev} = \frac{V_{vol}(t)}{V_{vol,\infty}} \tag{1}$$

$V_{vol}(t)$ and $V_{vol,\infty}$ son las cantidades acumuladas de volátiles emitidas hasta el momento t y hasta el final de la devolatilización, respectivamente.

3. Resultados

En la figura 1 se muestran las producciones de carbonizado, condensables y gas obtenidas para los diferentes combustibles a diferentes temperaturas. Las cantidades en la gráfica se han referido la cantidad de C, H y O en el material seco sin ceniza alimentado al reactor.

Se puede destacar que para todos los combustible, la producción de carbonizado es coherente con la fracción de carbono fijo medida durante el análisis inmediato. Según estudios presentados en la literatura la producción de carbonizado está estrechamente relacionada con la composición de la biomasa, especialmente con el contenido en lignina. También puede influir la presencia de diferentes especies inorgánicas y esto podría ser importante sobre todo en el caso de materiales con un alto contenido de cenizas como los lodos de depuradora.

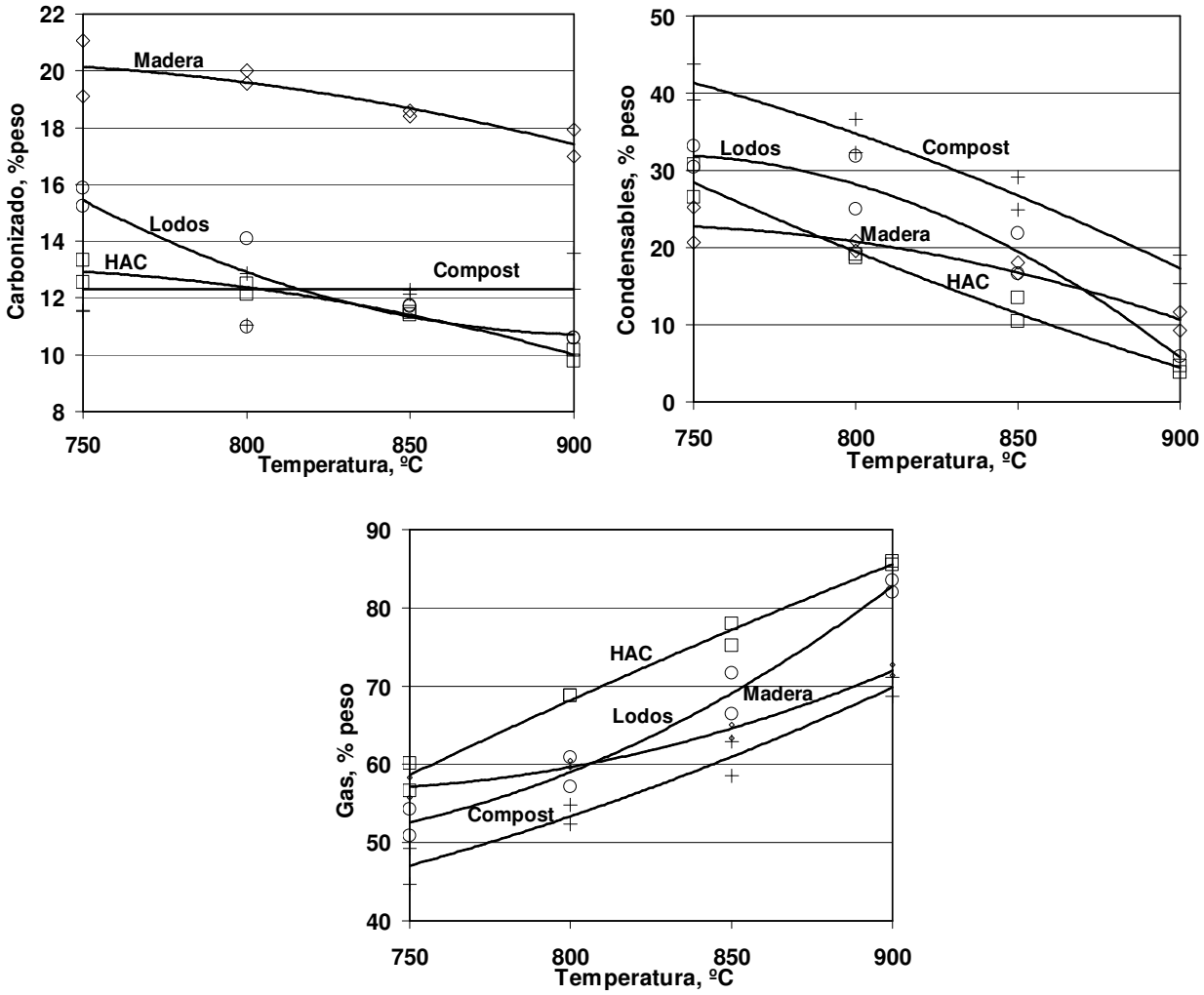

Figura 1: Producciones de carbonizado, condensables y gas obtenidas durante la devolatilización de madera (◊), HAC (□), lodos (○) y compost (+) (velocidad de fluidización = 0.8 m/s).

Los resultados muestran que los componentes mayoritarios del gas producido durante la devolatilización son CO y CO_2, pero también se producen cantidades importantes de CH_4 y H_2. La composición del gas obtenido a partir de madera se diferencia en gran medida de los gases obtenidos a partir de los otros materiales. Para la madera, la concentración de CO en el gas es mayor que para las otras biomasas mientras que la concentración de CO_2 es menor y estos resultados concuerdan con datos de la literatura.

El tiempo de devolatilización para los diferentes materiales fue calculado como el tiempo necesario para alcanzar una conversión de 90% (x_{dev} = 0.90) y los resultados se muestran en la figura 2. Los resultados muestran que la devolatilización de compost es mucho más lenta comparado con los otros materiales, especialmente a temperaturas bajas, mientras que la conversión de madera es la más rápida. Por ejemplo, a 800 ºC, los tiempos de devolatilización fueron de 56 s, 74 s, 71 s y 159 s para madera, HAC, lodos de depuradora y compost respectivamente.

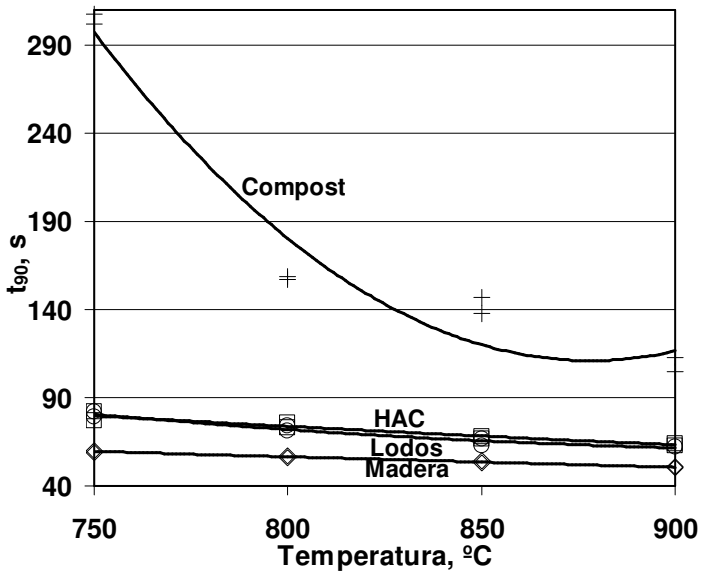

Figura 2: Tiempo de devolatilización, t_{90}, en función de la temperatura, para madera (◊), HAC (□), lodos (○) y compost (+) (velocidad de fluidización = 0.8 m/s)

Se llevaron a cabo varios ensayos para estudiar los efectos del tamaño de partícula durante la pirólisis de lodos de depuradora. Para los ensayos se emplearon partículas de 1.2 mm y de 4.5 mm y con las partículas más grandes se obtuvo más carbonizado y menos gas y la conversión fue más lenta que con las partículas más pequeñas.

También se llevaron a cabo experimentos para estudiar los efectos de la cantidad de biomasa alimentada al reactor para llevar a cabo la pirólisis. Tanto para madera como para HAC 1, al aumentar la cantidad de biomasa alimentada, se obtuvo más condensable y menos gas. Esto podría deberse a que los flujos de volátiles son mayores y por lo tanto el tiempo de residencia de los volátiles dentro del reactor es menor. También se vio influenciada la composición del gas, siendo la concentración de H_2 mayor al alimentar más cantidad al reactor. Esto podría deberse a un aumento de la actividad de reacciones homogéneas dentro del reactor debido a que las concentraciones de las especies volátiles son mayores.

4. Modelado de la conversión de madera y lodos de depuradora

La temperatura a la que un material se devolatiliza depende de su composición y de la velocidad de calentamiento a la que se somete. Diferentes componentes de una misma biomasa se pueden descomponer a diferentes temperaturas.

Empleando números adimensionales se puede determinar si la velocidad de devolatilización está limitada por la cinética de devolatilización o por el calentamiento de la partícula y si el calentamiento está limitado por la transferencia de calor externa o interna. Si se cumple que Da>>1, se puede considerar que la devolatilización es controlada por el calentamiento de la partícula y si Da<<1, la devolatilización es controlada por la cinética de la descomposición de la biomasa. Da es el número de Damköhler, $Da=k_{dev}\rho c_p R^2/\lambda_{eff}$, siendo k_{dev} la constante cinética de la devolatilización

suponiendo que esta sigue una cinética de primer orden y λ_{eff} la conductividad térmica de la biomasa. También se puede definir el número de Biot, Bi=hR/k_{eff}, siendo h el coeficiente de transferencia de calor externa. Si Bi>>1, el calentamiento vendrá determinado por la transmisión de calor dentro de la partícula y existirán gradientes de temperatura importantes dentro de la partícula y si la cinética de devolatilización es rápida existirá un frente de devolatilización que separa la zona de material que ya se ha descompuesto térmicamente con otra zona sin reaccionar. Si por lo contrario se cumple que Bi<<1, se puede considerar que la transferencia de calor externa controla la velocidad de calentamiento y por lo tanto la temperatura dentro de la partícula será homogénea y la descomposición térmica tendrá lugar simultáneamente a lo argo de todo su volumen.

Una forma sencilla de determinar el fenómeno limitante de la velocidad de devolailización es medir experimentalmente el tiempo de devolatilización para diferentes tamaños de partícula. El tiempo de descomposición se puede ajustar a una expresión del tipo: t_{dev}=k·d_p^n. Si se obtiene que n=2, el fenómeno controlante es la transmisión de calor interna, mientras que si n=1, controla la transferencia externa de calor y si n=0, el proceso está controlado por la cinética de la devolatilización.

4.1 Desarrollo de un modelo de partícula

En este trabajo se ha desarrollado un modelo matemático para calcular la evolución de las temperaturas dentro de los pellets de madera y de las partículas de lodos a partir del momento en el que estas se alimentan al reactor. Para el modelo se ha tomado las siguientes simplificaciones: se supone que el secado no afecta al calentamiento de la partícula, se ha asumido que el calor de devolatilización es despreciable, se ha supuesto que en el reactor la transferencia de calor por radiación es despreciable frente a la convección, se ha asumido que las propiedades físicas del combustible se mantienen constantes durante la devolatilización y que el calentamiento de la partícula no se ve afectado por el flujo de volátiles que abandonan la partícula. Para el caso de pellets de madera se ha asumido que la transferencia de calor solo tiene lugar en la dirección radial. Tomando estas simplificaciones se puede calcular las temperaturas de la partícula sin tener en cuenta el proceso de devolatilización y el sistema de ecuaciones a resolver es el siguiente:

$$c_p \rho \frac{\partial T}{\partial t} = \lambda_{\text{eff}} \left(\frac{\partial^2 T}{\partial r^2} + \frac{b}{r} \frac{\partial T}{\partial r} \right) \qquad (2)$$

$$\frac{\partial T}{\partial r} = 0 \quad \text{at } r=0 \qquad (3)$$

$$\lambda_{\text{eff}} \frac{\partial T}{\partial r} = h(T_\infty - T) \quad \text{at } r=R \qquad (4)$$

$$T = T_0 \quad \text{at } t=0 \qquad (5)$$

Se han empleado diferentes correlaciones para determinar el coeficiente de transmisión de calor externa y existen diferencias importante entre los valores calculados con las distintas expresiones. Puesto que en un reactor de lecho fluido de laboratorio en el que

la biomasa se alimenta por la parte superior, es probable que la biomasa pase gran parte del tiempo en la parte superior del lecho, el coeficiente de transferencia de calor externa debería tomar valores intermedios entre los valores calculados para un lecho fluidizado y para una partícula en contacto con una corriente de gas sin la presencia de partículas inertes. Las propiedades físicas de lodos secos de depuradora y pellets de madera fueron tomadas de la literatura.

4.2 Simulación de la conversión de pellets de madera

En la figura 3 se muestra la evolución con el tiempo de las temperaturas en la superficie y en el centro del pellet, calculadas con el modelo, y la conversión, obtenida experimentalmente.

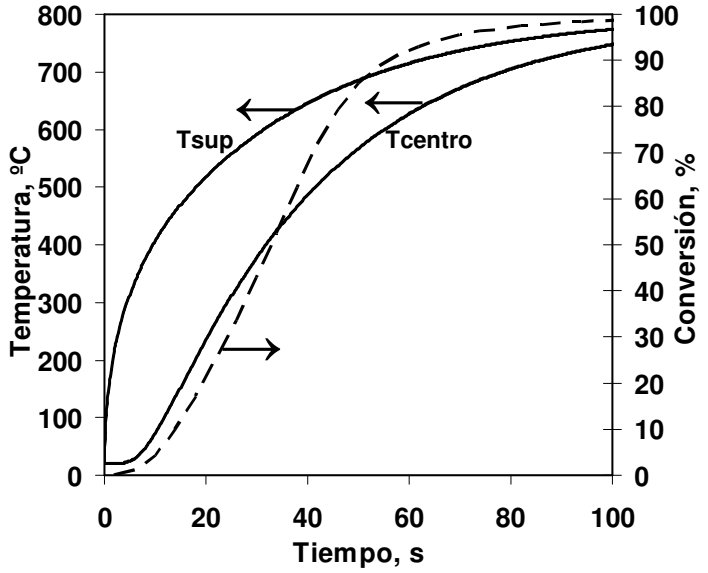

Figura 3: Temperaturas de la partícula, en la superficie (Tsup) y en el centro (Tcentro), calculadas con el modelo, y la conversión, obtenida experimentalmente, en función del tiempo, para una temperatura en el reactor de 800 ºC.

En la figura se puede ver que existen importantes gradientes de temperatura dentro del pellet durante la conversión, aunque también influye la transferencia de calor externa, ya que esta no es instantánea.

Las temperaturas del pellet calculadas se emplearon para simular las curvas de conversión frente al tiempo para diferentes temperaturas en el reactor. Otros autores han simulado la devolatilización de madera como una reacción instantánea que tiene ligar a una temperatura determinada. Las temperaturas de descomposición de los diferentes componentes de la madera se suele tomar a partir de medidas realizadas en termobalanza. El suponer que la devolatilización ocurre a una temperatura determinada es una simplificación ya que los estudios realizados en termobalanza muestran que la descomposición ocurre dentro de un rango de temperaturas y que las temperaturas de descomposición dependen de la velocidad de calentamiento. Existen numerosos estudios donde se han obtenido los coeficientes cinéticos y orden de reacción para la

devolatilización de madera y de sus componentes. Las cinéticas obtenidas en diferentes estudios difieren entre si. En este trabajo, para simular la descomposición térmica de madera, se ha empleada una expresión cinética que fue obtenida con un equipo experimental parecido al empleado aquí. En la figura 4 se muestran las curvas de conversión frente al tiempo calculadas y obtenidas experimentalmente para diferentes temperaturas en el reactor.

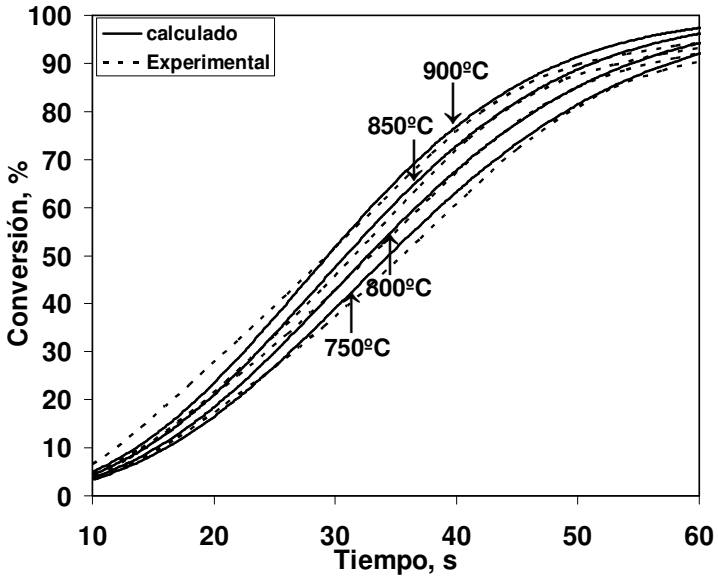

Figura 4: Conversión en función del tiempo durante la devolatilización de pellets de madera a diferentes temperaturas, curvas experimentales (líneas discontinuas), curvas calculadas a partir del modelo (líneas continuas).

Como se puede ver en la figura 3, el modelo es capaz de predecir razonablemente la conversión de pellets de madera a diferentes temperaturas.

4.3 Simulación de la conversión de lodos de depuradora

En la figura 4 se han representado las temperaturas en la superficie y en el centro de partículas de lodos de 1.2 y 4.5 mm calculadas con el modelo y las curvas de conversión frente al tiempo obtenidas experimentalmente.

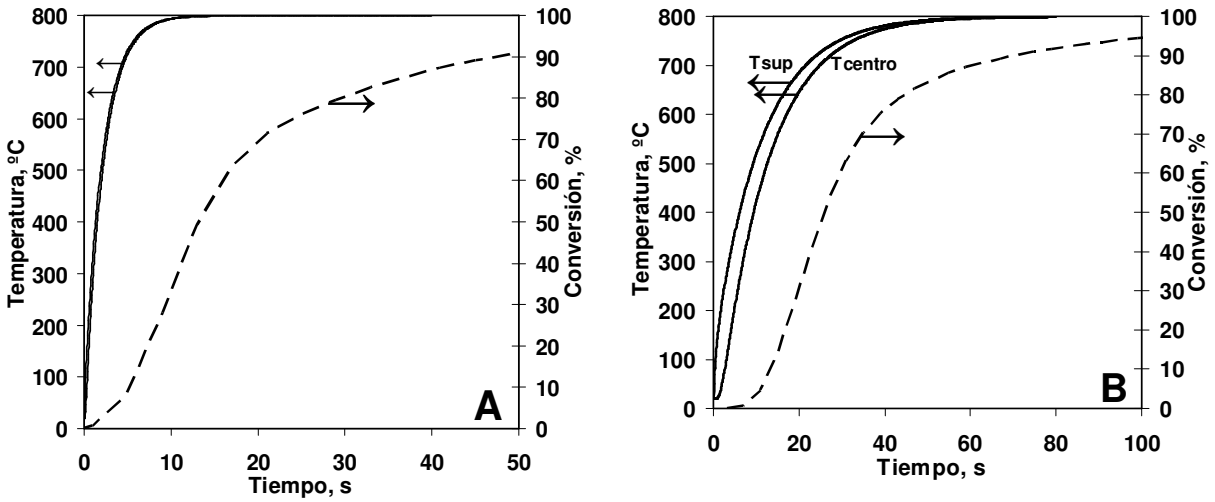

Figura 4: Temperaturas en la superficie y en el centro de la partícula calculadas con el modelo y curvas de conversión frente al tiempo para partículas de 1,2 mm (A) y de 4.5 mm (B). Temperatura en el reactor = 800 ºC.

De la figura 4A se puede concluir que para las partículas de 1.2 mm, el calentamiento es rápido comparado con la devolatilización y que la mayor parte de la conversión ocurre cuando la partícula ha alcanzado la temperatura del reactor. También se ve que para estas partículas, los gradientes internos de temperatura son despreciables. De esto se concluye que la devolatilización de lodos de 1.2 mm a 800ºC es controlada por la cinética y por lo tanto se podría obtener la cinética del proceso. Se emplearon los datos de conversión frente al tiempo obtenidos a 750 ºC y 800 ºC para obtener la energía de activación y el factor preexponencial para la devolatilización de lodos, suponiendo que esta sigue una reacción de primer orden. Para esto, se realizó la representación de t_{xdev} frente a $\ln(1/(1-x_{dev}))$ para las dos temperaturas, donde t_{xdev} es el tiempo necesario para conseguir una conversión, x_{dev}, determinada. Los resultados muestran que existen dos rangos de x_{dev} donde la relación entre t_{xdev} y $\ln(1/(1-x_{dev}))$ es lineal, pero en las dos zonas la ecuación de la recta es distinta. Es decir, a partir de una conversión de 0.70, la cinética de la reacción cambia. Esta modificación de la cinética a partir de cierta conversión se puede deber a varias razones. Una posible explicación es que el lodo esté compuesto por varias fracciones de materia con diferentes cinéticas de descomposición y por lo tanto las sustancias más reactivas se agotan antes lo que conlleva una modificación de la cinética global de devolatilización conforme avanza la conversión.

Los datos cinéticos obtenidos a partir de los experimentos con partículas de tamaño 1.2 mm, se emplearon para simular las curvas de conversión frente al tiempo para lodos sin tamizar (con un tamaño medio de 3.3 mm) y para partículas de 4.5 mm. El resultado se muestra en la figura 5.

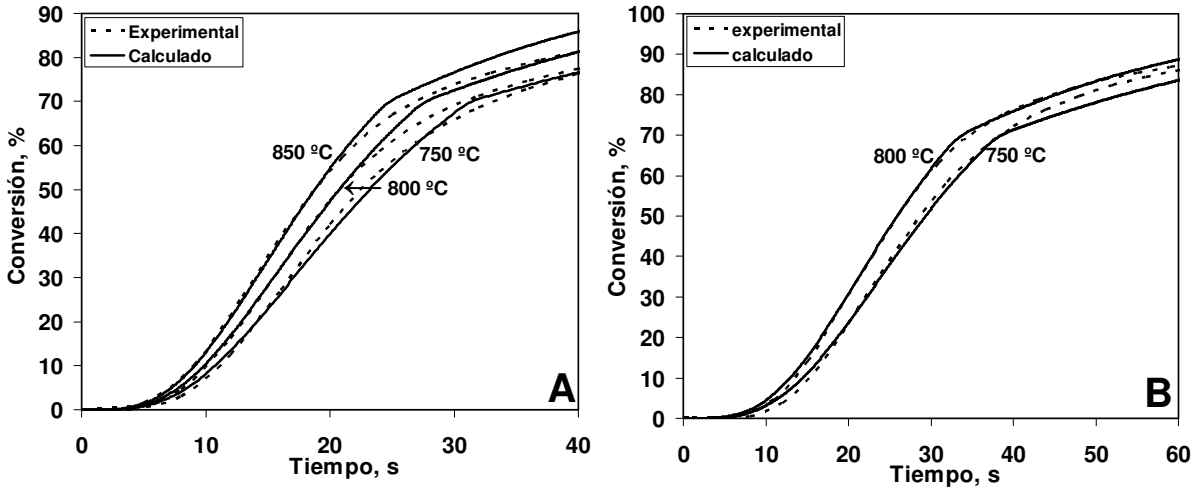

Figura 5: Conversión en función del tiempo durante la devolatilización de lodos de depuradora, (A) lodos sin tamizar, (B) partículas de 4. curvas experimentales (líneas discontinuas), curvas calculadas a partir del modelo (líneas continuas).

La figura 5 muestra que el modelo para lodos de depuradora es capaz de reproducir bien los resultados experimentales.

Según las figuras 4A y 4B las temperaturas a las que se devolatilizan las particulas de lodos de 1.2 mm y 4.5 mm son muy diferentes. Esto puede ser una razón por la que la distribución de productos de la pirólisis difiere para estos dos tamaños.

5. Conclusiones

Se ha estudiado la devolatilization de varios biocombustibles (madera, harinas cárnicas, compost y lodos secos de depuradora) en un reactor de lecho fluidizado de escala de laboratorio a temperaturas de entre 750 y 900 ºC. Se han determinado la cantidades de carbonizado, condensables y gas producidas, la composición del gas y el tiempo de devolatilización. Se ha desarrollado un modelo simple que permite conocer el modo de conversión de pellets de madera y partículas de lodos de depuradora. Se ha concluido que el calentamiento de las partículas de lodos está influenciado sobre todo por le transmisión de calor externa, mientras que en el caso de pellets de madera, la transferencia de calor dentro de la partícula es muy importante. Se concluyó que la devolatilización de partículas finas de lodos de depuradora estaba controlada por la cinética durante la mayor parte del tiempo y se obtuvieron los parámetros de Arrhenius para una cinética de devolatilización de primer orden. Estos parámetros cinéticos se emplearon para simular la conversión de partículas de lodos grandes con buen resultado.

5.1 Trabajo futuro

En esta sección de va a describir los trabajos futuros a realizar dentro del proyecto *FletGas* y en especial las que se desarrollan dentro de la tesis doctoral en la que está englobado el presente trabajo fin de master.

La próxima tarea a desarrollar es la realización de ensayos de pirólisis de lodos de depuradora durante las cuales no solo se van a medir las producciones de gas ligero y de carbonizado sino que se van a medir también agua y alquitranes. Se medirá tanto la cantidad total de alquitranes como su composición y esto permitirá comprobar los balances de carbono, hidrógeno e oxígeno. En este momento se está realizando ensayos de gasificación de carbonizado de lodos de depuradora con CO_2 y en un futuro próximo se va a medir también la reactividad de este carbonizado con vapor de agua. Los datos obtenidos durante los ensayos de pirólisis y de reactividad del carbonizado se van a incorporar a un modelo de gasificador desarrollado en Aspen Plus. Este modelo permitirá simular la temperatura del reactor, la cantidad de volátiles obtenidos y su composición, así como la conversión del carbonizado para diferentes caudales de entrada de combustible, aire, aire enriquecido y vapor. Este modelo servirá como apoyo para el diseño del una planta piloto.

Otra tarea a realizar es el modelado y simulación de un lecho móvil de char. Esta tarea se va a desarrollar durante una estancia en *Chalmers University of Technology*, Göteborg, Suecia, que comenzará en enero del 2010. Primero se desarrollará un modelo de una partícula de carbonizado que se empleará en el posterior desarrollo de un modelo de lecho de fijo que permitirá el cálculo de la conversión del carbonizado obtenida bajo

diferentes condiciones de temperatura, caudal y composición del gas de entrada y tamaño de las partículas del lecho y que servirá para el diseño del *chemical quench*.

Otra tarea a realizar es el desarrollo de un modelo fluidodinámico del sistema completo para lo que se realizarán ensayos en frío en una instalación ya existente. Esta instalación, que está hecha de metacrilato, consta de tres lechos fluidizados y un lecho fijo interconectados.

Una parte muy importante del proyecto trata sobre la conversión de los alquitranes, por lo que se realizarán ensayos tanto de generación primaria como de reactividad secundaria. Se estudiará como se ve influenciada la cantidad y composición de los alquitranes generados por la velocidad de calentamiento y por el tamaño de partícula. Los datos obtenidos servirán para desarrollará un modelo de pirólisis de una partícula para poder escalar los resultados a otras condiciones de operación. También se realizarán ensayos de conversión secundaria de alquitranes y se establecerá la reactividad de estos en diferentes condiciones de temperatura y atmósfera circundante. Los datos obtenidos, tanto durante los ensayos de pirólisis como de conversión secundaria se incorporarán en un modelo de devolatilización en lecho fluido que junto con los datos de reactividad del carbonizado permitirá el desarrollo de un modelo detallado de gasificación en lecho fluidizado.

El acoplamiento del modelo de lecho fluidizado con el modelo del *Chemical Quench* permitirá la simulación del sistema completo, que combinado con ensayos realizados en planta piloto servirá para la optimización del diseño y operación del sistema para diferentes combustibles.

1. INTRODUCTION

1.1 Introduction

Biomass gasification is a technology of great interest because of the benefits of transferring the calorific value from a solid fuel to a gas. The produced gas can be employed in clean and efficient applications, such as co-firing in existing boilers and, when sufficiently cleaned, engines and turbines generating electricity. Gasification of renewable fuels, such as biomass fuels and residues is of special interest, because they present environmental benefits compared to coal gasification and other fossil fuel applications.

Biomass gasification projects present problems derived form high raw material costs and poor stability in the fuel supply. Gasification of wastes and residues has gained enormous interest in recent years, because it does not present the aforementioned drawbacks of biomass gasification, given its low, zero or occasionally even negative cost and the ability to guarantee the fuel supply for large plants, with the following advantages of the economy of scale and guaranteed operation during the whole year. Residues such as sewage sludge and fractions of different municipal solid wastes, wastes and rests from animals, etc., have been considered as energy sources in the lasts years. An important drawback for the use of these residues in boilers is the contamination of the resulting gas. The incineration of residues is generally not desirable since the incineration of some residues can lead to high concentrations of dioxins and furans in the outlet gases. The shortage of oxygen during the gasification

process limits the formation of these species. In addition, in gasification processes, smaller volumes of gases are produced leading to less expensive gas cleaning.

1.2 Gasification in fluidized bed

Fluidized bed biomass gasification presents a great number of advantages compared to gasification in fixed beds, especially regarding possibilities for scale-up, automation and adaptability to different biomasses and residues and it is thus especially efficient for industrial processes employing these kinds of fuels. This technology has been demonstrated in the last years through a number of international projects on heat and electricity generation.

Gasification of biomass and wastes in fluidized bed presents two major drawbacks, the low carbon conversion achieved under practical operation conditions, due to the poor char conversion, and the high tar concentration in the outlet gas. The tar contained in the product gas can cause a series of problems in downstream equipment. Condensation of these compounds can cause clogging of exit pipes, particulate filters, fuel lines and injectors in internal combustion engines, etc. and it can cause corrosion in downstream equipment. In pressurized combustion engines, erosion caused by soot formation can occur. In order to avoid condensation of tars the temperature has to be maintained at a value above the dewpoint of the gas. The required conditioning of the gas depends on its application. Many applications require the gas to be compressed before the end-use equipment, for example gas turbines, and before the compression the gas needs to be cooled down.

The elimination of tars from the product gas still presents certain technical and economical difficulties. Different methods have been employed for tar removal; physical removal, thermal cracking, catalytic cracking, partial oxidation or deposition on a bed of porous particles[1].
Physical removal of tars implies the loss of the chemical energy contained in these compounds. This method applies wet scrubbing and filtration to remove the tars and implies the generation of large quantities of wastewater. ECN, The Netherlands, has developed a new physical removal process named OLGA, in this process the condensed tars are removed from the scrubbing liquid and recycled to the gasifyer, nevertheless, this technology is not feasible for small scale applications due to is complexity and high costs.
Thermal cracking is a hot cleaning method that requires temperatures above typical gasifier exit temperatures (>1100 ºC) to achieve high conversion efficiencies. In addition, thermal cracking can produce soot which is an unwanted impurity in the product gas.
A great deal of work on catalytic conversion of tar has been carried out in recent years In these applications the required temperatures are lower than for thermal cracking, but operation costs are high since the employed catalysts are expensive and deactivate after a relatively short period of time.
Primary methods for tar elimination, such as the use of in bed catalysts and secondary injection have also been investigated, but they have not shown to be efficient enough to be employed as stand alone methods for tar removal[2].

The low conversion of char in fluidized bed gasification due to the continuous removal of bed material and due to entrainment of fine char particles from the bed. The endothermic char gasification reactions are slow compared to the other processes, and high temperatures are required to attain reasonable char conversion.

1.3 Scope of this work

The Bioenergy group of the University of Seville has gained great experience in the field of fluidized bed gasification of biomass and wastes over the last eight years. Work has been developed at both laboratory, pilot and demonstation (3 MWth) scale. At the moment, work is being developed within a project called *FletGas*, where a new gasification technology is being developed.

The new technology is developed in order to overtake the aforementioned drawbacks of fluidised bed gasification. It is a gasification concept based on a three stage gasification process: a FB devolatiliser, an air/steam reforming of the gas coming from the devolatiliser, and the chemical quench of the unconverted char drainaged from the FB. Under this concept, the char and the tar are converted in two sequential stages which anables a high degree of flexibility and heat integration. The system permits optimization of primary and secondary conversion of tars by steam injections at different locations together with independent temperature control for the different sections. This process can tolerate very different types of biomass and blends by adjustment and optimisation of process variables.

The main task of the project is the construction of a pilot plant for the technical demonstration of the proposed concept. Further tasks are the development of models and the scaling-up of the process for the simulation of this technology under different scales. This includes the economical evaluation of various gasification plants at different scales representing small and medium plants for distributed power production from biomass and residues. Another important objective is to study the primary generation and secondary transformation of tars under different process conditions.

Two PhD theses are developing within the frame of this project. The first of these theses is focused on the study of primary generation and secondary conversion of tars in the different units that comprise the gasification system. The quantity and composition of the tars generated at different temperatures and heating rates is investigated. Also the secondary conversion of these compounds under different operating conditions; temperature, composition of surrounding gas, bed material employed and fluidodynamics in the bed is studied.

The second thesis, where this master thesis is included, aims at the development of a detailed reactor model that permits the simulation of the entire gasification system. The model developed will thereafter be employed to optimize the operating parameters and design of the different parts of the system. In order to achieve the objectives of this thesis, separate models for each unit need to be developed. Kinetic data obtained during the development of this project need to be incorporated into such models. The sub-models will thereafter be incorporated into a global model to simulate the system as a whole.

A basic fluidized bed gasifier model has already been developed, but a devolatilization sub-model based on experimental data needs to be incorporated. This master thesis is aimed at obtaining such experimental data for a number of different fuels.

1.4 Summary of the different sections in this work

In the next section, the theoretical aspects of devolatilization are treated. The most important parameters that affect the process are discussed and a summary of results found in literature is presented.
The section that follows, deals with the experiemtal work. The employed experimental rig employed is presented. A short introduction to the different fuels employed is made and a detailed description of the experimental procedure and treatment of data is also included.
In section 4, the experimental results are presented and these results are compared to data found in literature. The effects of different operating parameters are discussed and simple correlations for predicting product yields and gas composition as a function of temperature are obtained.
In section 5, a simple particle model is developed to predict the mode of conversion of wood pellets and DSS granulates of different sizes. Simulations are carried out to validate the model and a more simple model for calculating the devolatilization time is presented.
In the last section, the conclusions obtained from this work are outlined and a brief description of future work to be carried out within the *FletGas* project is

2. THEORETICAL ASPECTS OF DEVOLATILIZATION

2.1 Introduction

In the following, theoretical aspects of the devolatilization of biomass and wastes will be treated. Also a short summary of literature data is presented.

Devolatilization is a key conversion stage during gasification and combustion of biomass fuels. Knowledge of yields and composition of volatiles is especially relevant for high volatile fuels such as biomass and waste. When biomass is devolatilized, light gases and tars represent 70–90 wt% of the total mass fed, whereas only 10–30 wt% is char[1]. In a fluidized bed (FB) gasifier, the yield of char is useful to determine the bed size of the gasifier and the carbon conversion and efficiency achieved in the reactor. Determination of tar yield is essential since high tar content limits the gas application. On the other hand, in FB combustion, mixing of oxygen and volatiles from fuel particles during devolatilization affects the combustion efficiency and emissions.

The products of devolatilization of biomass are usually lumped into light gases which include CO, CO_2, H_2, CH_4 and other light hydrocarbons, liquid, including tars and water and char. Char is a carbonaceous solid that remains after thermal decomposition. Apart from the ash contained in the fuel, the char may also contain high-molecular-weight tar compounds[3].

Different laboratory devices have been used to characterize devolatilization: packed bed furnace[2], thermogravimetric apparatus (TGA)[4, 5], or FB[6, 7]. TGA is usually employed when devolatilization kinetics are to be obtained. In TGA, very small samples and very fine particle sizes are used and the heating rates are low (typically 5-40 ºC/min). Under these conditions, heat transport limitations are minimized, which is a necessary condition when measuring pyrolysis kinetics. Drop tube furnace has also been applied to obtain devolatilization kinetics at temperatures above 450 ºC[3]. Much kinetic data on biomass devolatilization has been published over the years although there is great variation between the data given by different authors.

2.2 Parameters affecting devolatilization

Devolatilization experiments are usually conducted in inert atmosphere, using N_2 and He as carrier gas for the evolving volatiles. During devolatilization, the produced volatiles are transported out of the fuel particle by convetive flux[3]. This convective flux enables the volatils to be carried away from the particle before reacting with the surrounding gas and it prevents contact between the surrounding gas and the fuel particle. Consequently, devolatilization occurring inside a gasifier or a combustor can be described by experiments carried out in inert atmosphere.

Studies on biomass and waste found in literature show that the product yields depend to a large extent on the composition of the material employed, the particle size and the way of operation, mainly temperature and heating rate[8,9]. The product distributions obtained during devolatilization are a function of both the primary generation due to the thermal decomposition of the fuel and secondary reactions involving the produced volatiles. Secondary reactions may occur homogeneously or heterogeneously, both inside the fuel particle and in the reaction furnace.

Primary generation is influenced mainly by the composition of the fuel and by the heating rate applied to the particle. The product distribution obtained from various types of biomass has been studied as a function of the cellulose, hemicellulose and lignin contents[4,5,10,11]. Catalytic effects of different mineral compounds may also influence the product yields.

An increase in heating rate has shown to give lower char yields[12]. Thermal decomposition of wood has commonly been expressed as a single process, including three parallel reactions for char, tar and liquid formation, the so-called “Shafizadeh” scheme[3]. The kinetic parameters were obtained by regression of yield versus temperature data. The calculated activation energies are lower for char formation than for liquid and gas formation, predicting successively lower char yields as the temperature increases.

Secondary tar reactions include thermal cracking, reforming and polymerization reactions leading to soot formation. Also water-gas shift reaction may occur.

Particle size influences the heating rate and thus the distribution of primary devolatilization products. Particle size can also influence the product distribution through secondary intraparticle volatiles reactions. For thermally thin particles, where no temperature gradients are present, drying and devolatilization occur in sequence and

homogeneously throughout the particle, while for thermally thick particles, important intraparticle temperature gradients exist and the processes of drying an devolatilization may occur at different times in different parts of the particle, and this enhances contact between evolving moisture and volatiles during devolatilization and in addition, the volatiles have to pass through a hot char layer before leaving the particle. Intraparticle tar reactions have been found to reduce liquid yields[13,14]. Char has been found to enhance thermal cracking of tars[15] leading to the formation of more char. When looking at the influence of particle size, one has to keep in mind that the volatiles generation during devolatilization can produce high pressures within the particle, which can lead to fragmentation of large particles.

The extent of extraparticle thermal cracking of tars is influenced by both temperature and gas residence time. These reactions are important at temperatures above 500-600ºC. And at high temperatures they may occur to a significant extent even for residence times as low as 0.1 s[16]. During pyrolysis experiments, inert carrier gas is supplied to the system in order to minimize the extent of thermal cracking and homogeneous gas phase reactions, by reducing the gas residence time and the concentrations of volatiles species in the reactor.

The initial mass fuel of fuel employed in the experiments can influence the product yields due to a decrease in gas residence time as a consequence of an increase in the rate of volatiles release. Also homogeneous gas phase reactions such as the water-gas shift reaction may be enhanced as a consequence of the increased volatiles concentration inside the reactor.

2.3 Literature study

Many pyrolysis studies have been carried out for wood[7,8,15,17,18,19]. Comparatively less work exists on characterization of contaminated biomass, residues and wastes[20,21,22]. Pyrolysis studies found in literature usually report yields of char, tar and gas as well as main gas species, although, sometimes yields of water and different inorganic contaminants and composition of tar can also be found. Both DSS and MBM have high nitrogen and sulphur contents compared to biomass and the formation of contaminating species, such as NH_3, HCN and SH_2 may be significant. During DSS pyrolysis in fluidized bed, more than 50% of the fuel nitrogen has been found to produce NH_3 and HCN[22].

A number of different devolatilization studies presented in literature were reviewed for comparison with our results. There are a great number of studies on wood pyrolysis available, while the amount of work treating devolatilization of wastes is much more limited. For example, for compost no data was available and for MBM, no data obtained in FB could be found. In table 1 information from the different works is give. It includes information about the biomass studied, the most relevant results and a description of the reactor furnace employed.

Comparing the results obtained with different reaction furnaces for wood pyrolysis, it was found that while the char yields were very similar, the gas yields were higher when the pyrolysis was carried out in a FB. Also the gas compositions given by different authors differ considerably, especially regarding the CO_2 concentration. The gas

composition can be modified to a large extent due to secondary tar conversion, which is dependent on temperature, particle size, gas residence time etc. and due to homogeneous gas phase reactions. Results obtained with DSS in FB[23] showed that the CO and CO_2 concentrations in the gas can differ considerably between different sewage sludges, and the differences were attributed to variations in the composition of the organic matter contained in DSS. The results from this study were not included in table 1 because the authors did not give information about the reactor temperature during the experiments.

Source	Temperature, °C	750	810	850	Biomass	Reaction furnace	Observations
24	Char yield	22.3			DSS	Fluidized Bed	Continuous DSS feed rate of 40kg/h.
	Oil yield	21.1					
	Gas yield	40.8					
	Water yield	8					
	CO vol%	33.9					
	CO2 vol%	8.5					
	CH4 vol%	27.6					
	H2 vol%	30.0					
25	Char yield			19.9	Anaerobically Digested DSS	Fixed bed	Heating rate = 60°C/min. The CO_2 yield decreased with increasing temperature.
	Liquid yield			55.6			
	Gas yield			26.0			
	CO vol%		35.8				
	CO2 vol%		1.7				
	CH4 vol%		12.5				
	H2 vol%		50.0				

Table 1: Results from devolatilization of biomass and wastes presented in literature.

(The table continues on the next page.)

Source	Temperature, ºC	750	800	865	900	910	Biomass	Reaction furnace	Observations
26	Char yield	25					Pine sawdust	Fluidized bed	
	Liquid yield	18							
	Gas yield	57							
27	Char yield		17.5		15		Sawdust	Stirred pyrolysis furnace connected to a cracking reactor	No inert gas was introduced at temperatures above 200ºC
	Liquid yield		40		37.5				
	Gas yield		42		45				
28	Char yield			22.1		22.1	Wood chips	Fixed bed	
	Liquid yield			50.2		51.2			
	Gas yield			23.6		25.6			
	CO vol%			41.1		43.3			
	CO2 vol%			40.0		36.4			
	CH4 vol%			12.7		13.6			
	H2 vol%			6.10		6.67			
29	Char yield		20.5		18		Wood	Quartz tube with a basket sample holder, and a steel-ring-filled cracking zone.	CO2 yield decreased with increasing temperature
	Tar yield		11		7.5				
	Water yield		22.5		20				
	Gas yield		44.8		46				
	CO vol%		53.2		55.8				
	CO2 vol%		9.7		5.2				
	CH4 vol%		15.1		12.6				
	H2 vol%		22.1		26.4				

Continuation of, **Table 1:** Results from devolatilization of biomass and wastes presented in literature.

(The table continues on the next page.)

Source	Temperature, ºC	750	800	900	Biomass	Reaction furnace	Observations
30	Char yield		18.8	13.9	Launan chips	Fluidized bed	Microspherical alumina particles used as inert bed material
	Liquid yield		17.3	10.4			
	Gas yield		63.8	75.6			
	CO vol%		41.2	45.5			
	CO2 vol%		33.1	22.9			
	CH4 vol%		14.0	13.1			
	H2 vol%		11.7	18.5			
31	Char yield		18.4	18.4	Holm-oak wood sawdust	Stainless steel reactor with a wire mesh basket sample holder	The char yield was independent of the particle size at 500 ºC
	Liquid yield		28.1	25.0			
	Gas yield		53.5	56.0			
32	Char yield	17.6	16.4	15.8	MBM	Fixed bed	Heating rate = 8ºC/min
	Tar yield	58.2	57.6	58.2			
	Gas yield	22.2	25.2	25.3			
	CO vol%	16.8		18.1			
	CO2 vol%	39.1		38.8			
	CH4 vol%	14.0		11.2			
	H2 vol%	30.2		31.9			

Continuation of, **Table 1:** Results from devolatilization of biomass and wastes presented in literature.

2.4 Devolatilization models

A devolatilization model aims at obtaining the rates of generation of the different volatile products, as well as the yields of char, tar, light gas and water and the composition of the tar and gas fractions. Many different reaction schemes have been used to describe devolatilization. The most simple models represent pyrolysis by a single reaction or by a combination of series and parallel reactions. First order kinetics

of the different reactions is commonly used, although nth order expressions have also been employed[33]. Also distributed activation energy models where the activation energy is described by a continuous distribution function have been applied to fuel devolatilization[34]. These models can be applied to obtain yields of tar, gas and char, but they do not predict the composition of volatiles. The models have been employed together with detailed transport models (particle models) to predict devolatilization times and product yields, but Wang et al.[35] concluded that it is not possible to accurately predict product yields for biomass pyrolysis from the available kinetics. Other more complicated structural models have been developed for prediction of yields and composition of the main products, recently reviewed by[36].

Detailed particle models are not frequently used for fluidized bed simulations. Instead semi-empirical and or simplified particle models are used. Simplified models estimate the time of complete devolatilization by considering the rate-limiting phenomena. The yields of char and volatiles and the composition of volatiles are not predicted but they are estimated separately by empirical relations based on experimental data together with mass balances[37]. Empirical data or particle models can be applied to FB models together with some limiting cases for mixing. For instance, in a bubbling FB gasifier, when the vertical transportation (segregation) of fuel particles is rapid compared to devolatilization, most of the devolatilization takes place at the bed surface because it is assumed that the particles keep floating once they have reached the bed's surface. In such a case, the gas produced is directly influenced by the gas yields obtained by devolatilization. In the other limiting situation, when the devolatilization is rapid compared to vertical fuel mixing, most of volatiles are released in the bottom zone of the bed[21]. In this case, the gas from devolatilization can be considered as initial gas conditions for the process all the way up the bed. In both limiting situations, one mechanism, either reaction or mixing is dominant, and the devolatilization yields are used as boundary condition in the proper position (bed surface or bottom). To identify the limiting situations, the time of devolatilization has to be estimated and compared with the time of solid mixing. These times can be estimated employing experimental results obtained in laboratory and taking into account the effects of scale-up. As discussed in section 2.2, there are many factors that affect the product yields from devolatilization and care should be taken when selecting experimental data for gasifier simulations. For fluidized bed simulations, the employed devolatilization data should be obtained at high heating rates and due to the different behaviour of one biomass compared with another, even at the same operating conditions in an FB, extrapolation data from one biomass to another (and from coal) is questionable[36].

2.5 Conclusions

Devolatilization is a complex process that is influenced by many different factors. As a consequence, theoretical prediction of pyrolysis yileds is a complex task and therefore empirical data obtained in dedicated devolatilization experiments are usually employed in gasifier models. Special care should be taken when selecting experimental data, especially regarding the composition of the fuel, the heating rate and the extent of extraparticle secondary reactions. At high reactor temperatures, minimization of secondary reactions is a complex task and in many cases laboratory furnaces employed in devolatilization experiments have gas residence times above 0.5 s

In this work, experimental results useful for FB gasification and combustion simulations for wood and various wastes will be presented. Yields of char, tar, and volatiles, the composition of light gas as well as the time of devolatilization, were experimentally determined in a laboratory FB for different fuels and empirical correlations for predicting these parameters as a function of temperature are presented. The data provide a mean for direct comparison of the devolatilization behaviours of the different fuels studied. Also the fragmentation behaviour during devolatilization and combustion was analyzed for the different fuels. The fragmentation behaviour is important for predicting entrainment of material in a fluidized bed. It also affects the char particle size distribution which has a great influence on char oxidation and gasification reactions. Modelling of the devolatilization of a single particle was made for understanding the mechanisms that control the devolatilization rate and to provide a simple tool for estimating the devolatilization times in cases where the operating parameters differ from those employed in this study.

3. EXPERIMENTAL

In this section, the different fuels employed in this study will be presented. Also the experimental setup and test procedure are described in detail.

3.1 Material

Table 1 shows the chemical characterization of the six fuels used in this study. Commercial wood pellets cylindrically shaped with a mean diameter of 6 mm were used. The bulk density of the wood pellets was 600 kg/m^3 and the particle density was 1300 kg/m^3. The MBM and compost from municipal solid waste (MSW) were received as powders and pellets were made for each material. Pellets were prepared manually by compacting 1 g of MBM together with 0.56 g of water and 2.1 g of compost respectively in a cylindrical mould with a diameter of 1 cm. The pellets made were dried in an oven at 105ºC during approximately 20 hours before being used in the experiments. Dried anaerobically digested sewage sludge (DSS) was received from an industrial drying plant processing the sludge from sewage treatment plants. Table 2 shows the particle size distribution of the DSS as received. The particle density was 1450 kg/m^3, whereas the bulk density was 760 kg/m^3. As received DSS comprises roughly 98% (mass basis) in the size range of 2.00−4.00 mm. In this work the size range 4.00-5.00 mm (average 4.5 mm) was studied as representative of behavior of the largest DSS granulates. In addition, a finer range 1.00−1.40 mm (average 1.2 mm), was studied to represent the conversion of fine granulates and to obtain kinetic parameters.

3.2 The rig.

Figure 1 shows the experimental setup. The reactor is a batch operated lab-scale bubbling FB. It consists of three parts: a preheating section, a reaction part (bed), and the freeboard. The reactor is made of refractory-lined stainless steel tubes of AISI-316 and with different diameters; 26.6 mm ID in the reaction zone and 52 mm ID in the freeboard zone. The height of the bed is 150 mm and the height of the freeboard is 200 mm. The distributor plate is drilled with 27 holes having 1 mm ID. The preheating section, bed and freeboard are surrounded by an electrical 4.6 kW_e furnace, controlled to obtain the desired reaction temperature. The reactor is equipped with one thermocouple (K-type) and two pressure taps as indicated in Figure 1.

Downstream of the reactor, the gas passes through a line with different units for gas cleaning (see Figure 1). The aim of the gas cleaning line is to avoid deposition of tar compounds within the probe and to protect the gas analyzer. The composition of the gas was measured continuously by a Siemens analyzer using a non-dispersed infrared method for CO, CO_2 and CH_4 measurements and thermal conductivity and paramagnetic methods for H_2 and O_2 measurements, respectively. The signals from the analyzer are transmitted to the computerized data acquisition system, where they are monitored and registered.

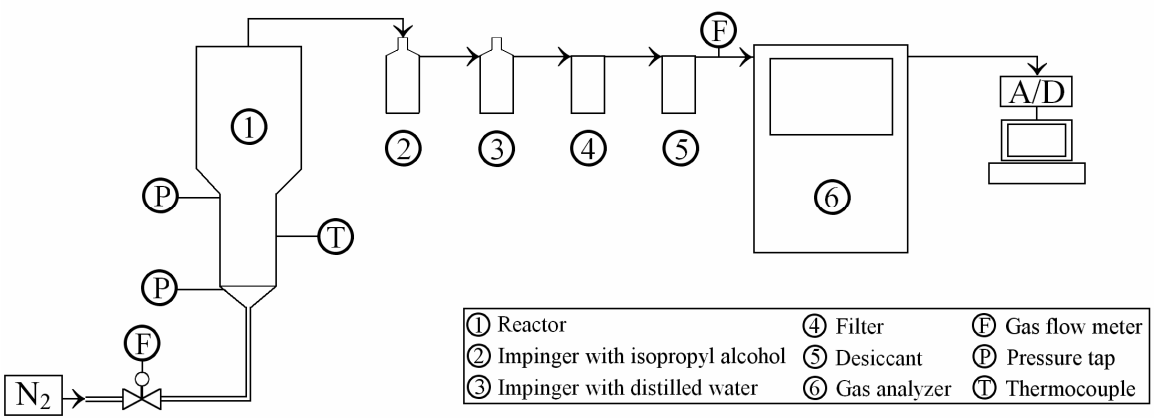

Figure 1: Experimental setup

	Wood pellets			DSS granulates			MBM			Compost		
	As received	Dry basis	Dry ash-free basis	As received	Dry basis	Dry ash-free basis	As received	Dry basis	Dry ash-free basis	As received	Dry basis	Dry ash-free basis
LHV (MJ/kg)	17.08	18.39	18.52	11.18	12.47	21.94				9.20	13.21	14.16
HHV (MJ/kg)	18.42	19.65	19.79	12.25	13.41	23.59				10.42	14.01	15.02
C %wt	-	49.47	49.80	-	30.88	54.32	-	50.27	55.75	-	33.78	56.03
H %wt	-	5.79	5.83	-	4.36	7.67	-	7.30	8.10	-	3.71	6.15
N %wt	-	2.03	2.04	-	4.76	8.37	-	11.51	12.76	-	1.83	3.04
S %wt	-	0.06	0.60	-	1.24	2.18	-	0.53	0.59	-	0.68	1.13
O %wt	-	41.94	42.22	-	15.61	27.46	-	20.56	22.80	-	20.29	33.66
Moisture %w	6.28	-	-	8.65	-	-	4.70	-	-	25.62	-	-
Ash %wt	0.67	0.71	-	39.42	43.15	-	9.37	9.83	-	29.54	39.71	-
Volatiles %w	75.89	80.98	81.56	47.28	51.75	91.03	77.35	81.16	90.01	39.86	53.59	88.89
Fixed C %w	17.16	18.31	18.44	4.66	5.10	8.97	8.59	9.01	9.99	4.98	6.70	11.11

Table 1: Chemical characterization of the fuels investigated.

Sieve size (mm)	Mass fraction
> 5	0.75
4 – 5	0.28
2.8 – 4	54.86
2 – 2.8	39.44
1.4 – 2	3.70
1 – 1.4	0.71
0.5 – 1	0.21
< 0.5	0.05

Table 2: Particle size distribution of as received DDS

3.3 Operating conditions

Experiments were conducted varying reactor temperature, fluidizing velocity, particle size and the size of the fuel batch. Table 3 shows the different operating conditions studied for each material. Normally 1 g batch of fuel has been used, although, for experiments conducted on DSS and compost, batch sizes above or equal to 2 g were used given the low amounts of volatiles released by these materials. The particle size of DSS particles was also varied. Two fluidizing velocities, 0.55 and 0.8 m/s were studied for DSS to asses the effect on the results and to verify that entrainment of material from the FB was limited. The amount of ofite used in all experiments was 35 g.

Material	Temperature, °C	Fluidizing gas velocity, m/s	Batch size, g	Particle size[b],mm
Wood	750, 800, 850, 900	0.8	1, 2	25, 12.5
MBM	750, 800, 850, 900	0.8	1	Approx. 15
DSS	750, 800, 850, 900	0.55, 0.8	2	As received, 1.2[a], 4.5[a]
Compost	750, 800, 850, 900	0.8	Approx. 2.1	Approx. 20

[a] **Average particle size.**
[b] **Pellet length or granulate diameter**

Table 3: Operating conditions studied for the different materials

3.4 Test procedure

The procedure used for each experiment was the following:

1. A batch of 35 g of ofite was introduced into the reactor.
2. The FB reactor was heated by the electrical furnace to the desired test temperature under continuous flow of pure nitrogen.
3. The volumetric flow of nitrogen was adjusted to establish the desired fluidizing velocity.
4. A batch of fuel was injected down to the bed by two ball valves, falling through a stainless steel pipe situated 150 mm above the distributor plate. The length of the

tube was kept short so that the material reaches the bed after a very short period of time.

5. The devolatilization process was monitored until no CO, H_2, CO_2 or CH_4 were detected in the gas (3-10 minutes depending on the material being devolatilized).
6. At the end of the tests, air was fed into reactor to burn the remaining char.

In some tests, the bed was quenched by adding cold nitrogen together with switching off the oven. This was made to visualize the fragmentation patterns of the fuels during various stages of conversion.

3.5 Treatment of data

A blank test was made prior to the devolatilization experiments to assess the delayed time and dispersion in the gas measurements. The lag time that passes from the moment the volatiles are produced until they are detected by the gas analyzer was measured by injecting CO_2 at a certain moment during fluidization of the bed with N_2. Figure 2 presents the information acquired from the blank test. The step input is displayed by the dotted line whereas the dashed line represents the response to the CO_2 concentration. The steady state CO_2 concentration was between 30 and 40 %, which is a typical value employed when studying the kinetics of char gasification with CO_2. The curve fitted to the points in Graph (a) represents the theoretically calculated CO_2 molar fraction given by a dynamic model adjusted to the experimental data. The analytical expression of the transfer function G(s) is also included in the graph, from which it is seen that first order dynamics were assumed. From G(s) it is seen that the delay time for refreshment of gas when the supply line is switched from N_2 to CO_2-N_2 is roughly 40 s and the time constant 6.57 s. Graph (b) includes the curves C(t) and E(t) obtained from the experimental outlet of Graph (a). The dimensionless dispersion coefficient calculated from curve E(t) was 0.009, indicating that back-mixing in the system is limited and that correction of the experimental concentration curves is only needed with regard to the lag time, which was subtracted from the observed conversion times.

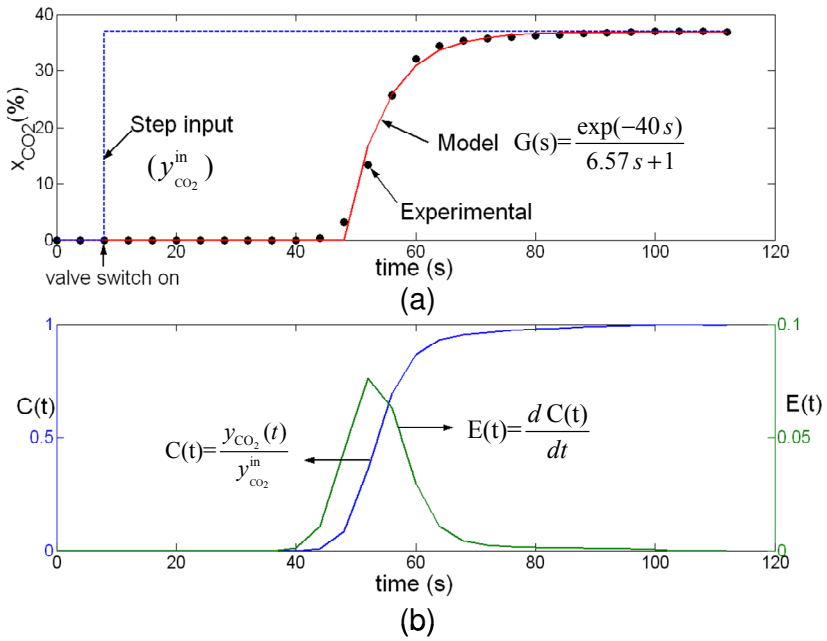

Figure 2: Blank test output.

The char, condensate and gas yields were referred to the carbon, hydrogen and oxygen contained in the dry fuel free of ash. The amount of char remaining after devolatilization (char yield) is calculated through the carbon in the gas detected in the combustion stage by measuring the carbon in the CO and CO_2. The gas yield (overall or accumulated) of different species was calculated as the accumulated amounts of CO, CO_2, CH_4 and H_2 detected by the analyzer during devolatilization. The condensate yield was calculated by difference and thus it includes, tar, water and light hydrocarbons not measured (all except for the CH_4). In the temperature range studied in this work, variations of the pyrolytic water yield (that formed during devolatilization excluding the fuel moisture) and light hydrocarbons are expected to be small compared to that of tar[38, 29]. As a result, variations in condensate yield can be considered to be caused by variations in the tar yield. Since the condensate yield is not measured, it is not possible to check the mass balances, although the reported results for wood are consistent with data on yields of water and composition of tar found in literature.

The progress of devolatilization is traced by the degree of particle conversion, x_{dev} defined as [39]

$$x_{dev} = \frac{V_{vol}(t)}{V_{vol,\infty}} \quad (1)$$

$V_{vol}(t)$ and $V_{vol,\infty}$ being respectively, the accumulated mass of volatiles measured up to a time t and that after complete devolatilization. The experimental devolatilization time t_{xdev} is calculated as the time to achieve x_{dev}.

In the next section, the experimental results will be analyzed in detail.

4. EXPERIMENTAL RESULTS AND DISCUSSION

In this section the experimental results are presented and compared to results found in litterature. The differences between the results obtained with different fuels are discussed briefly and the effects of different operating parameters are analyzed. The mode of conversion is analyzed for wood pellets and DSS particles by employing a simple particle model.

Figure 3 shows the pictures of the various fuels prior to devolatilization and the corresponding char obtained after devolatilization. In the case of DSS, the ash obtained after complete combustion is also shown. The figure provides a qualitative judgment of the fragmentation behavior during devolatilization of the fuels tested. MBM pellets (Figure 3 (a)) showed severe fragmentation during devolatilization. The original shape and volume of the pellet was reduced during devolatilization and a recognizable skeleton was no longer observed at the end of the process. This observation is in agreement with previous works[20,40] reporting the poor structural durability of pellets produced from MBM. Wood pellets (Figure 3(b)) were subjected to significant shrinking during devolatilization while fragmentation was neglected during this period. Fragmentation was observed during combustion of the char, specifically at high conversions (not shown in the picture). Compost pellets (Figure 3(c)) behaved similarly to wood pellets: they reduced their volume during devolatilization, while the original shape was maintained and no fragmentation was observed. The original shape and size of DSS granulates was observed to remain after both devolatilization and combustion (Figure 3(d)). These observations agree well with the findings by[27, 28, 29] that showed the

skeleton of the DSS granulates to be stable and to maintain their original shape despite the fluidizing action of the bed.

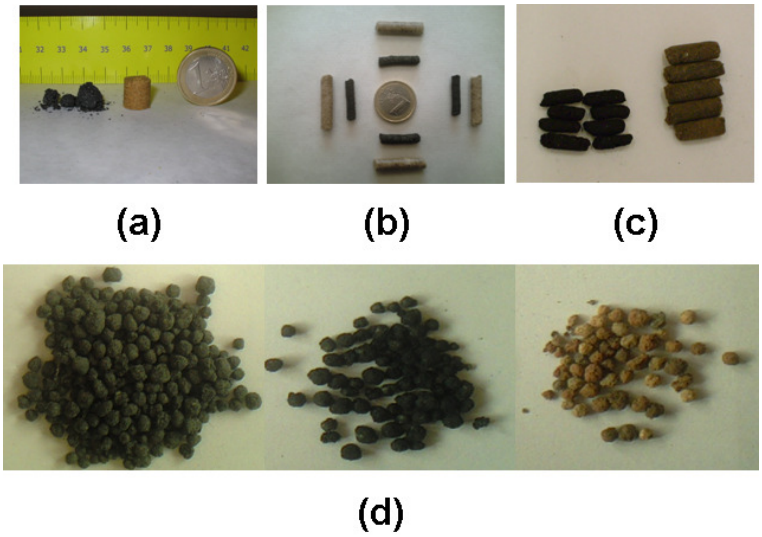

Figure 3: Pictures of (a) Meat and bone meal pellet and the char generated after devolatilization. (b) Wood pellets and the corresponding char obtained after devolatilization at various temperatures. (c) Compost pellets and char after devolatilization. (d) DSS granulates (as received), char after devolatilization and ash after complete combustion.

Figure 4 shows the char, condensate and gas yields as a function of temperature for the fuels tested. As expected[7,17,41], the gas yield increases with temperature, whereas the condensate and char yield decrease for all fuels. Though, the char yields varied less with temperature than the condensate and gas yields.

For wood, the decrease with temperature of the condensate yield was less pronounced than for the other materials, consistent with previous work[41], arguing that the tar from wood is less reactive than tar from various agricultural residues. Somewhat similar conclusions were made in[18], observing that some tars from the pyrolysis of wood were practically unaltered even under very severe conditions (high temperature and residence time).

The char yield from wood pellets and grape seed were the highest, roughly 20 wt% whereas the MBM and DSS were the fuels with most gas release. For MBM, the amount of condensate was practically zero at 900ºC. The higher char yields obtained from wood and grape seed compared to the other materials are consistent with their significantly higher fixed carbon content (21.2% wet basis for grape seed). The char yield is expected to be closely related to the biomass composition, especially to the lignin content[41,42,43,44] though, the presence of different inorganic species and physical properties, such as particle density and thermal conductivity, may also affect the product yields[42,45,46]. The high ash content in DSS and the presence of metals could favor gas formation at expenses of char formation [23].

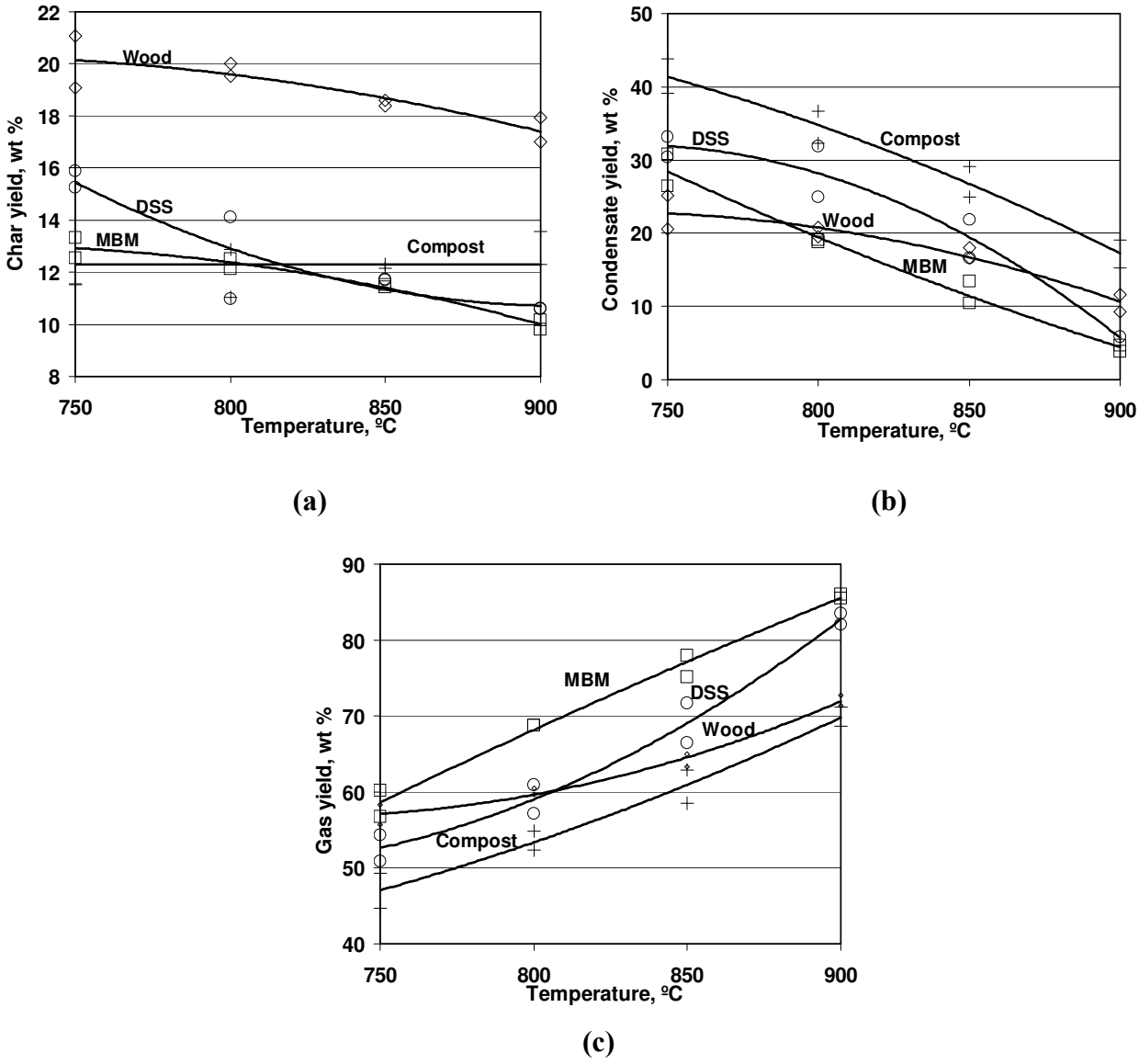

Figure 4: Yields of char (a) condensate (b) and gas (c) obtained during the devolatilization of wood (◊), MBM (□), DSS (○), compost (+) and Grape seed (—) (u = 0.8 m/s).

For all the materials studied, the char yields obtained were close to the fixed carbon content (daf basis) given by the proximate analysis (see Table 1).

The repeatability was reasonable for all fuels with the exception of compost. The lower repeatability of compost was attributed to the heterogeneity of the received material. This can also explain unexpected results such as the observed slight increase in char yield with increasing temperature (Figure 4(a)).

The volume fractions of the main species in the gas (CO, CO_2, CH_4 and H_2) obtained from the different materials is shown in Figure 5. Wood gave higher CO concentrations and lower CO_2 concentrations in the gas than the other materials. These observations are in agreement with those given in[41], where higher CO yields and lower CO_2 yields were measured for wood, compared to various agricultural residues.

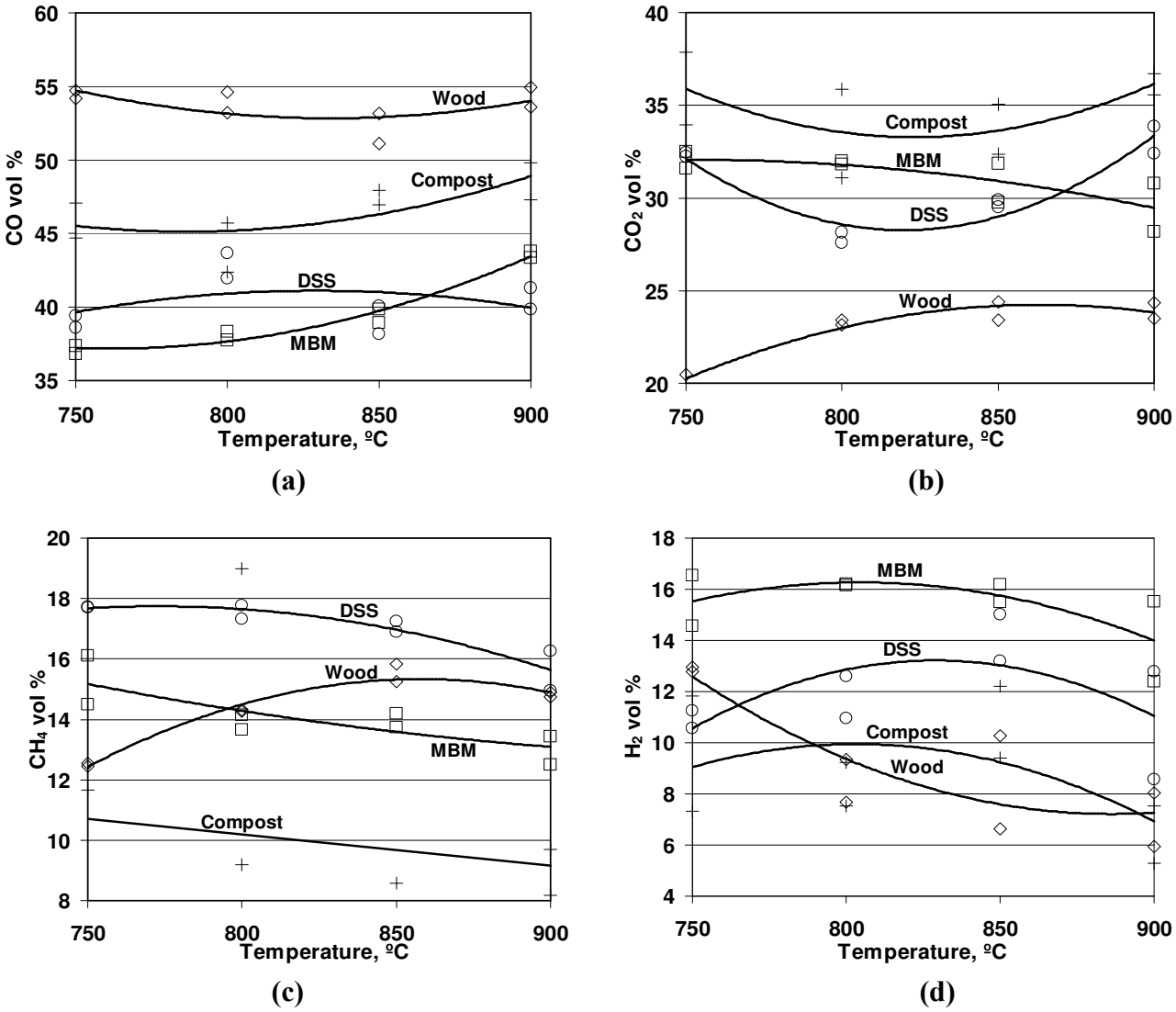

Figure 5: Experimental composition of the main components in the gas (volume fraction): CO (a), CO_2 (b), CH_4 (c) and H_2 (d), during the devolatilization of wood (◊), MBM (□), DSS (○) and compost (+) (u = 0.8 m/s).

The char, tar and gas yields, as well as the CO, CO_2, CH_4 and H_2 volume fractions in the light gas, were fitted to a quadratic function of temperature (T in ºC):

$$f(T) = a_0 + a_1\left(\frac{T}{T_{ref}}\right) + a_2\left(\frac{T}{T_{ref}}\right)^2 \qquad (2)$$

The values of parameters a_0, a_1 and a_2 for T_{ref} = 500ºC are shown in Table 4. Jiang et al.[36] gave a similar correlation for corncobs in an FB in the temperature range of 650–850 ºC.

	Char yield, wt%			Condensate yield, wt%			Gas yield, wt%		
	a_0	a_1	a_2	a_0	a_1	a_2	a_0	a_1	a_2
Wood	-15.03	50.58	-18.09	-196.07	300.86	-103.34	311.10	-351.45	121.43
MBM	- 30,26	60,92	-21,42	75,89	20,00	-34,46	54,38	- 80,92	55,87
DSS	167.23	-172.39	47.47	-705.63	981.52	-326.63	757.85	-959.74	326.52
Compost	26.35	-21.76	7.94	-32.71	157.47	-72.06	106.36	-135.71	64.12

	CO volume %			CO2 volume %			CH4 volume %			H2 volume %		
	a_0	a_1	a_2	a_0	a_1	a_2	a_0	a_1	a_2	a_0	a_1	a_2
Wood	240.53	-225.12	67.50	-206.86	267.66	-77.50	-168.64	214.47	-62.51	234.97	-257.01	72.50
MBM	227,59	- 249,96	82,04	-19.28	69.40	-23.44	38.73	-22.51	4.53	-160.70	220.28	-68.53
DSS	-119.25	193.38	-58.30	561.00	-649.90	198.21	-60.13	100.77	-32.60	-281.62	355.75	-107.31
Compost	226.21	-230.24	73.19	363.60	-401.28	121.88	18.37	-5.12	0.00	-197.17	257.93	-80.30

Table 4: Values of parameters a_0, a_1 and a_2 of the quadratic fits as a function of temperature of char, tar and gas yields and gas compositions.

The conversion time t_{90} obtained for the different materials, calculated as the time needed for 90% of the total amount of gases to evolve, is shown in Figure 6(a). As expected, the conversion times decreased with increasing temperature. Compost gave significantly longer conversion times than the other biomasses, especially at lower temperatures, while wood presented the lowest values. In Figure 6(b) the compost has been removed allowing clearer observations of the t_{90} for wood, MBM and DSS. The influence of the moisture content on the devolatilization times is expected to be small since the moisture content of wood and DSS is low and MBM and compost were dried before the tests.

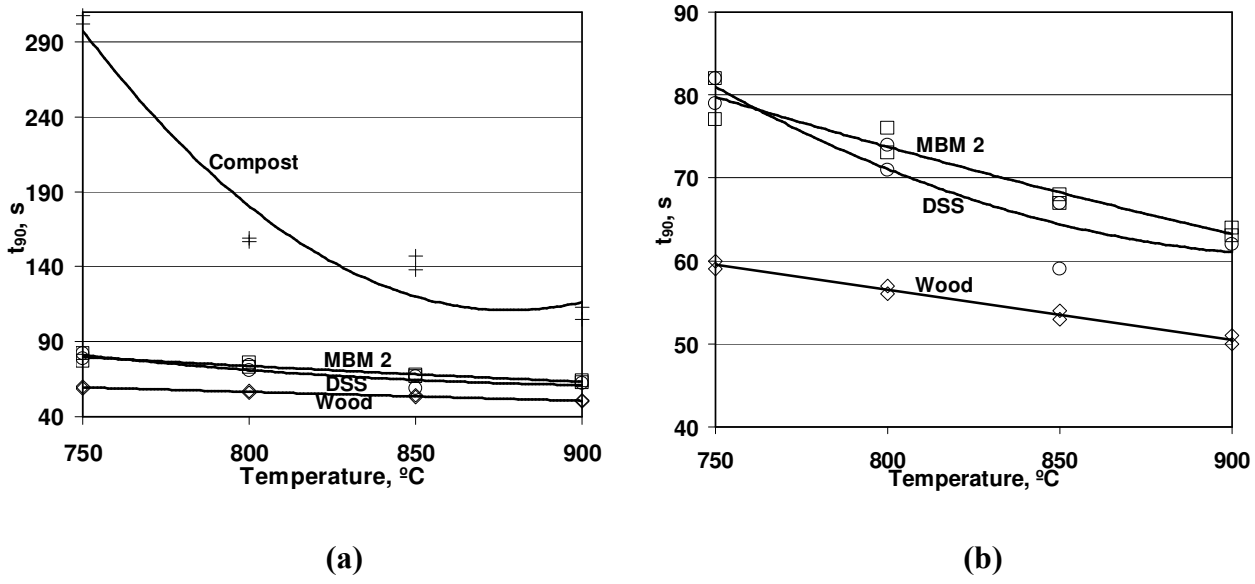

Figure 6: Times for 90% conversion, t_{90}, for wood (◊), MBM (□), DSS (○) and compost (+) (u = 0.8 m/s).

The effect of particle size on the results was studied for the DSS granulates. Figure 6 shows the char (Figure 6(a)) and gas (Figure 6(b)) yields obtained for the two particle sizes of DSS, 1.2 mm and 4.5 mm. The larger particles gave somewhat higher char yields and slightly lower gas yields, in agreement with previous works[18, 47].

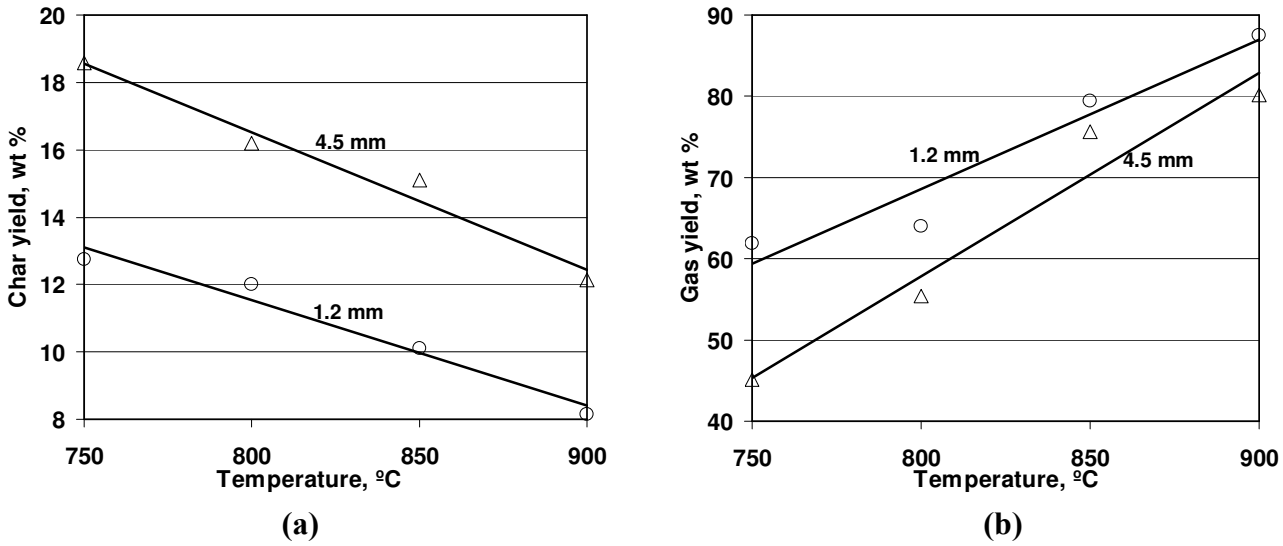

Figure 7: Effect of particle size and temperature on the yields of char (a) and gas (b) for DSS (u = 0.8 m/s).

In Figure 8 the time to reach 60% conversion, t_{60}, for three particle sizes of DSS (as received, 1.2 mm and 4.5 mm) is represented as a function of temperature. It is concluded that the effect of particle size is more significant than the temperature. The choice of t_{60} instead of t_{90} was made because the determination of the time to reach high conversion above 80% leads to higher scattering of measurements (this also occurred in[21]). The effect of particle size on the composition of the gas was small.

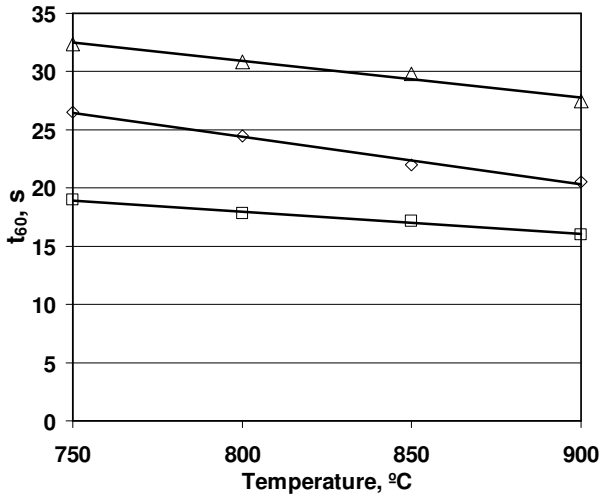

Figure 8: Time for 60 % conversion, t_{60}, for DSS as a function of temperature; DSS as received (◊), 1.2 mm particles (□) and 4.5 mm particles (Δ).

For the wood pellets, the diameter was kept constant (6 mm), but the length of the pellet was varied. Several tests were carried varying the pellet length maintaining the batch size and no significant effects were found on product yields or on conversion times.
The effect of the batch size was also studied to assess the effect on the yields and composition of the gas. For wood and MBM1, an increase in batch size from 1 g to 2 g had a slight effect on the results: the gas yields decreased while the condensate yields increased, especially at higher temperatures and this increase was more pronounced for MBM than for wood. The increase in condensate yield could be caused by a decrease in volatiles residence time due to higher rate of volatiles release. The composition of the gas was slightly affected by an increase in batch size, the H_2 concentration increased considerably at temperatures above 750ºC, while the concentrations of CO and CO_2 decreased, probably due to the enhancement of secondary gas-phase reactions.

The char, tar and gas yields presented in this work for wood agree well with the results obtained by other authors in FB[27, 30] (see Table 1). Also the char yield obtained by Chen et al.[41] show that the char yield is close to the fixed carbon content of the fuel.

In the next section, a simple particle model for assesment of the mode of conversion of wood pellet and fine and large DSS particles will be developed.

5. THEORETICAL ANALYSIS OF THE PROCESS

A simple model is developed to study the mode of conversion of a single fuel particle during devolatilization of DSS and wood in an FB.

5.1 Model development

The devolatilization of a particle is thermally driven. The evolution of the field of temperature within the particle is described by the partial differential equation of transient heat conduction with heat sources. Here, it is considered that the heat of pyrolysis is small[21,39] and that the fuel moisture does not affect the particle heat up due to the low moisture content of the fuels analyzed (see Table 1). In this way the temperature distribution during heating up of a particle can be approximately calculated without considering the thermal effects of pyrolysis and drying. Additional assumptions are: the heat flux due to the convective mass flux associated with the volatiles released is neglected[38]; the fuel properties and the particle size are assumed to remain constant during devolatilization and equal to those of the virgin biomass. Previous work has shown that the effects of particle shrinkage are small[48] and the effects caused by variations in specific heat capacity (c_p) and density (ρ) during the devolatilization are assumed to compensate each other (ρ is lower for the char than for the virgin wood, whist c_p of char is higher than that of wood[49]). After these simplifications the temperature field at different times is obtained by solving:

$$c_p \rho \frac{\partial T}{\partial t} = \lambda_{\text{eff}} \left(\frac{\partial^2 T}{\partial r^2} + \frac{b}{r} \frac{\partial T}{\partial r} \right) \tag{3}$$

$$\frac{\partial T}{\partial r} = 0 \quad \text{at } r=0 \tag{4}$$

$$\lambda_{\text{eff}} \frac{\partial T}{\partial r} = h\,(T_\infty - T) \quad \text{at } r=R \tag{5}$$

$$T = T_0 \quad \text{at } t=0 \tag{6}$$

where T_0, T_∞ are, respectively, the initial (ambient, 20ºC) and the bed temperature. b is a geometric factor, being equal to 0 for an infinite slab, 1 for an infinite cylinder and 2 for a sphere. The solution can be expressed in the form:

$$\Theta(T_{dev}) = \frac{T_b - T(r,t)}{T_b - T_0} = f\left(\text{Bi}, \text{Fo}\right) \tag{7}$$

Fo is the Fourier number defined as Fo= $k_{\text{eff}}\, t/(\rho c_{\text{p}} R^2)$ and Bi is the Biot modulus for heat transfer, defined as Bi=hR/k_{eff}. R is the radius in spherical and cylindrical particles whereas it is half of the thickness in a flat particle.
Once the temperature is known, the local conversion X_{dev} defined as $X_{\text{dev}}=(\rho_0-\rho)/(\rho_0-\rho_\infty)$, is calculated assuming a first order global reaction to describe the loss of mass by pyrolysis:

$$\frac{1}{(1-X_{dev})} \frac{\partial X_{dev}}{\partial t} = \frac{1}{(\rho - \rho_\infty)} \frac{\partial \rho}{\partial t} = -k_{dev} \tag{8}$$

where k_{dev} is a kinetic constant following the Arrhenius form:

$$k_{dev} = A_{\text{dev}} \exp\left(-\frac{E_{\text{dev}}}{R_g T} \right) \tag{9}$$

The conversion x_{dev} is finally obtained by integrating the local degree of conversion, throughout the particle

$$x_{dev}(t) = \frac{b+1}{R^{b+1}} \int_0^R r^b X_{dev}(r,t)\, dr \tag{10}$$

To obtain the evolution of x_{dev} with time during conversion, the model represented by eqs 3–6 and eqs 8-10 was integrated numerically and the calculation method is explained in the Appendix.

Various kinetic data of k_{dev} for wood and DSS pyrolysis are shown in Table 6. Olive residue is also included as representative of other biofuel materials. As seen, there is a great variation even for wood. This is explained by the way to obtain the kinetics by different researchers and also because the representation of pyrolysis by a first-order

global expression is a rough approximation. As a result the choice between one expression and another is difficult. This is discussed below for the specific fuels simulated.

Source	Fuel	E_{dev} (J/kmol)	A_{dev} (1/s)	k_{dev} (1/s) 500°C	800°C
(48)	Wood	$1.78\ 10^{8}$	$1.90\ 10^{12}$	$1.8\ 10^{0}$	$4.2\ 10^{3}$
(47)	White fir	$1.05\ 10^{8}$	$2.64\ 10^{5}$	$2.1\ 10^{-2}$	$2\ 10^{0}$
(6)	Beech wood	$2.05\ 10^{7}$	1.5	$6.2\ 10^{-2}$	$1.5\ 10^{-1}$
(49)	Sawdust	$1.83\ 10^{8}$	$1.00\ 10^{13}$	$4.3\ 10^{0}$	$1.2\ 10^{4}$
(50)	Olive residue	$1.14\ 10^{8}$	$3.27\ 10^{6}$	$6.6\ 10^{-2}$	$9.3\ 10^{0}$
(51)	DSS	$2.84\ 10^{8}$	$1.86\ 10^{19}$	$1.2\ 10^{0}$	$2.8\ 10^{5}$

Table 6: First-order kinetics models of pyrolysis for various fuels.

The effective gas-particle heat transfer coefficient, h, is calculated by considering only convection, a reasonable approximation under the conditions tested[50]. Two different correlations have been used to calculate h: The generally used Ranz and Marshall equation[42] given in eq (11) as well as a specific correlation derived for fuel conversion in FB (eqs (12) and (13)) [51, 52]. For wood pellets and for 4.5 mm DSS granulates, eq (12)[51,52] has been used, valid for large particles being converted in a FB of fine inert material. For 1.2 mm DSS granulates, eq (13)[51,52] has been applied, developed for particles of similar size to that of the inert bed particles in an FB.

$$\mathrm{Nu}_p = 2 + 0.6\,\mathrm{Pr}^{1/3}\,\mathrm{Re}_p^{1/2} \tag{11}$$

$$\mathrm{Nu}_i = 0.85\mathrm{Ar}_i^{0.19} + 0.006\mathrm{Ar}_i^{0.5}\,\mathrm{Pr}^{0.33} \tag{12}$$

$$\mathrm{Nu}_p = 6 + 0.117\mathrm{Ar}_i^{0.39}\,\mathrm{Pr}^{0.33} \tag{13}$$

As visualized in Figure 2, the MBM pellets were subjected to strong fragmentation and could not be analyzed under the simple model developed. For the compost pellets the uncertainty in its kinetics and the lack of thermo-physical data made it not possible to make a theoretical analysis of the process. As a result, in the following the model is applied for wood pellets and DSS granulates.

5.2 Scaling analysis

Firstly, scaling estimation through dimensionless numbers is made to preliminary assess if limiting mode of conversion during FB devolatilization of wood pellets and DSS granulates can be identified using data from literature. This is done by computation of Biot modulus for heat transfer, Bi, and Damköhler for devolatilization, Da_{dev}[39]. Bi, defined as $\mathrm{Bi}=hR/k_{eff}$, quantifies the thermal behavior of the fuel particles by comparing the rates of external and internal heat transport, respectively $h/(\rho c_p R)$ and $\lambda_{eff}/(\rho c_p R^2)$. If $\mathrm{Bi}\gg 1$, the particle heating is limited by intapartle heat transfer and if $\mathrm{Bi}\ll 1$, the external heat transfer is rate limiting. For comparing the particle heat up and the

devolatilization kinetics, when Bi>1, the Damköhler number of pyrolysis, defined as $Da_{dev}=k_{dev}\rho c_p R^2/\lambda_{eff}$, that compares the rates of pyrolysis kinetics, k_{dev}, and internal heat transfer is caulated and when Bi<1, Da_{dev}/Bi, which compares the rates of pyrolysis kinetics and external heat transfer is used. The Da_{dev} value depends on the temperature at which k_{dev} is calculated. Since the temperature at which devolatilization occurs is not known a priori, Da_{dev} is usually evaluated at the bed temperature.
The properties used for wood pellets and DSS are shown in Table 7. The properties for wood pellets were obtained from[53], where commercial wood pellets with similar size were converted in an FB. The density of DSS granulates was taken from [54], while the specific heat capacity and thermal conductivity of DSS were estimated assuming the thermal diffusivity of DSS to be intermediate between those of wood and silica[21]. Table 7 also includes the properties of the fluidizing gas, nitrogen, at 800ºC.

Property	ρ, kg/m^3	c_p, J/(kgK)	λ_{eff}, W/(mK)
Wood pellets	1300	1800	0.26
DSS	2000	1150	0.6

Nitrogen (800ºC)

ρ_G, kg/m^3	μ_G, kg/(ms)	λ_G, W/(mK)	Pr
0.32	$4.46\cdot10^{-5}$	0.071	0.705

Table 7: Thermo-Physical properties of wood pellets and DSS and properties of nitrogen at 800ºC.

The Nusselt number, Nu, obtained from eqs (11)-(13) and the corresponding *h* and Bi values calculated for wood pellets and DSS with 0.8 m/s gas velocity, at 800ºC, are shown in Table 8. Since the wood pellets are cylindrically shaped, the particle diameter was replaced with Ψd_{eq} in eq (11), being d_{eq} the equivalent diameter, $d_{eq} = (6V_p/\pi)^{1/3}$ and Ψ the particle sphericity, $\Psi=\pi d_{eq}^2/S_p$. There are significant differences between the *h* obtained from eqs (11)-(13): Eq (11) is an expression developed for single-phase flow and the values given by this expression are expected to be lower than the actual *h* in FB, where heat transfer is enhanced by the circulation of inert particles[51]. Equations (12) and (13), on the contrary, give maximum Nu values at optimum fluidization velocity[51, 52]. The actual *h* values for the experiments in the present work is expected to be intermediate between the values given by eq (11) and eqs (12) and (13) because in a small lab FB with the feeding at the top, it is most likely that the fuel particles stay most of the time at the bed surface during devolatilization[36,53]. Also, the heat transfer coefficient may be different in small scale fluidized beds compared to larger scales due to differences in gas flow patterns, which affects the movement of solids.

	Nu			h, W/(m^{2}K)			Bi			Da_{dev}	Da_{dev}/Bi
	(eq 11)	(eq 12)	(eq 13)	(eq 11)	(eq 12)	(eq 13)	(eq 11)	(eq 12)	(eq 13)		
Wood pellets	5.89	3.08		46.67	356.46		0.54	4.11		12.21 – 1.0 10^6	
DSS, 1.2 mm	3.18		7.33	188.19		471.38	0.19		0.47		8.22 10^5 – 2.03 10^6
DSS, 4.5 mm	4.76	3.41		75.06	356.46		0.28	1.37			3.97 10^6 - 1.94 10^7

Table 8: Estimates for the scaling analysis: Nu, h, Bi, Da_{dev} and T_{dev} calculated for wood pellets and DSS using eq. (11)-(13) and a gas velocity of 0.8 m/s to calculate Nu and h and data from Tables 6 and 7 for temperature of 800 ºC to calculate Da_{dev}.

None of the two limiting situations given by Bi (Bi>>1 or Bi<<1) can be clearly established for the fuels and operating conditions tested in the present work (see Table 8). Rough guides can, however, be established: given the relatively low Bi number for DSS, the external heat transfer should have a significant influence on the particle heat up. Similar results were obtained in[21] by conducting DSS tests with particles sizes in the range of 0.65 – 8 mm. In contrast, given the relatively larger Bi obtained for wood pellets, the internal heat transfer will greatly influence the particle heat-up and large temperature gradients will be present during the devolatilization of wood pellets. This agrees with the results obtained by Leckner et al.[38].

To compare the rate of heat transfer with devolatilization kinetics, the Da_{dev} calculated using the kinetics from Table 6 and thermo-physical data from Table 7 is presented in Table 8. The ratio Da_{dev}/Bi for DSS particles was also calculated for the cases where Bi<1. For Da_{dev} and Da_{dev}/Bi , instead of a single value, a range of values is presented in Table 8, resulting from the various kinetics (four for wood and one for DSS) and the two values of *h*. As seen Da_{dev} is high for all cases, no matter what kinetics or correlation of *h* is used. The lower bound for wood Da_{dev} (12.21) is obtained using the kinetics given by Jand et al.[7], which yields the lowest k_{dev} at high temperatures (see Table 6). Note that Da_{dev} is computed at bed temperature so a temperature, T_{dev}, between T_0 and T_b where Da_{dev} becomes high is likely to exist, in other words, there is a T_{dev} ($T_{dev}<T_b$) above which devolatilization is very fast compared to the heat up of the particle. Pyrolysis can be considered complete when the particle centre has reached T_{dev}[39,53].

For, , t_{dev}. In this scenario, the devolatilization can be assumed to be completed once the particle (the center in case of thermally thick particles) has heated up to T_{dev} and the time of conversion can then be estimated by the time for heating a particle up to T_{dev}. This simplification can be especially useful for engineering applications, for which it is often enough to predict the time of complete devolatilization. The time needed for particle heat up can be calculated by making asymptotic approximation of the two coefficients appearing in the first term of the Fourier series of the exact solution in eq. 7[52, 53] to give:

$$t_{dev} = \tau_{ih} \frac{1}{\mu_1^2} \ln\left(\frac{\mu_2}{\Theta(T_{dev})}\right) \tag{14}$$

$\Theta(T_{dev})$ being the dimensionless temperature defined as

$$\Theta(T_{dev}) = \frac{T_b - T_{dev}}{T_b - T_0} \tag{15}$$

Expressions for calculating μ_1 and μ_2, (the two coefficients of the first term of the solution expressed in Fourier series) are shown in Table 11.

	$0 < Bi_h < 2$	$2 < Bi_h < \infty$
μ_1	$\sqrt{\frac{a_0 Bi_h}{1+Bi_h / a_1}}$	$\frac{a_3 Bi_h}{Bi_h + a_4}$
μ_2	$1+\frac{Bi_h}{a_2}$	$\frac{a_5 Bi_h}{Bi_h + a_6}$

	a_0	a_1	a_2	a_3	a_4	a_5	a_6
Plate	1	3	7	π/2	0.95	1.273	0.15
Cylinder	2	4	4	2.4048	1	1.602	0.35
Sphere	3	5	3.5	π	1.1	2	0.65

Table 11: Values of μ_1 and μ_2 from eq(16).

Equation (14) can be used for both fine and large particles. For thermally fine particles, however, intraparticle temperature gradients are negligible, and a simpler expression can be used to estimate t_{dev}:

$$t_{dev} = \tau_{eh} \ln\left(\frac{1}{\Theta(T_{dev})}\right) \tag{16}$$

To estimate T_{dev} the condition $Da_{dev}=1$ or $Da_{dev}/Bi=1$ is used:

$$T_{dev} = \frac{E_{dev}}{R_g \ln\left(A_{dev}\tau\right)} \tag{17}$$

τ being the characteristic time for heat up, estimated by eqs (18) or (19):

$$\tau_{eh} = \frac{\rho c_p 2R}{h} \quad \text{for} \quad Bi<1 \tag{18}$$

$$\tau_{ih} = \frac{\rho c_p (2R)^2}{\lambda_{eff}} \quad \text{for} \quad Bi>1 \tag{19}$$

Figure 16 compares t_{dev}/τ_{ih} calculated by the approximate and numerical solution for various values of Bi and two Θ_{dev}, showing that the approximation given in Eq.(14) is excellent for Θ_{dev} typical of FB fuel conversion at high temperature (combustion and gasification).

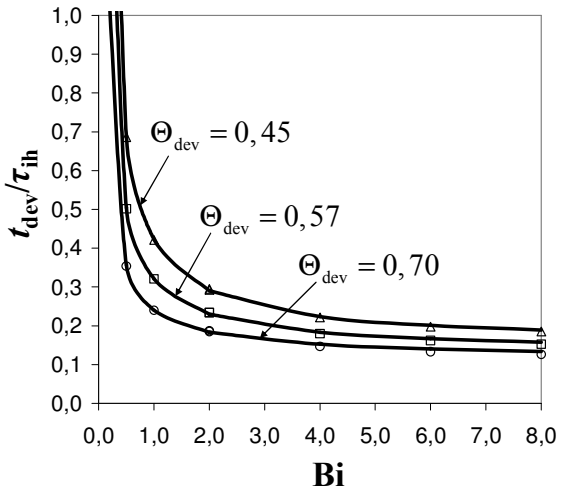

Figure 16: Comparison between t_{dev} calculated by the approximate and numerical solution for various values of Bi and two Θ_{dev}, typical of FB fuel gasification and combustion.

In Figure 17 t_{90} is calculated with the approximation using the various pyrolysis kinetics for wood given in Table 6[7,55¡Error! No se encuentra el origen de la referencia.,56,57] for comparison with the experimental t_{90} (bold spots). As seen, eq (14) gives a good prediction of t_{90} using the kinetics of Brink et al.[¡Error! No se encuentra el origen de la referencia.], whereas the agreement is poor when using the kinetics of Jand and Foscolo[6]. The use of Kosstrin's and Davidsson's kinetics yields intermediate results.

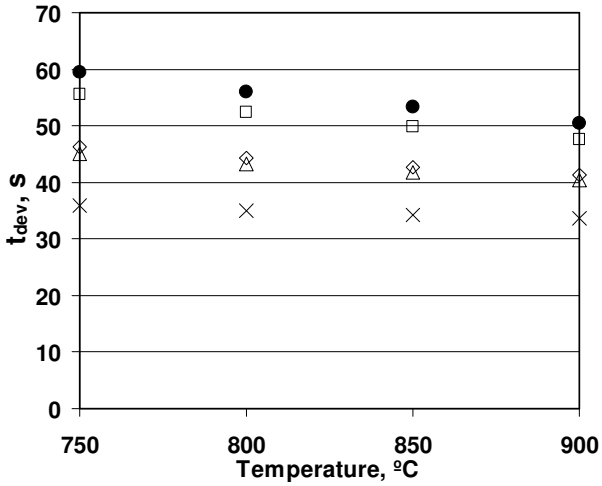

Figure 17: Comparison between t_{dev} obtained experimentally (●) and t_{dev} calculated from the approximate solution and employing devolatilization kinetics from literature: (◊) Davidsson et al. (54), (Δ) Kosstrin (55), (□) Brink (56), (×) Jand and Foscolo (6).

As explained, t_{dev} calculated from eq (14) is expected to be a good approximation for the devolatilization time as long as Da_{dev} changes rapidly with temperature once T_{dev} has

been reached, i.e. $d(\mathrm{Da_{dev}})/dT >> 1$ for $T \geq T_{dev}$. This is true as long as the activation energy of the pyrolysis reaction is greater than for heating. Since the latter is a physical process, with lower activation energy than a chemical process, the assumption is, in principle, reasonable. However, when pyrolysis is assumed to be described by a single first order reaction, the kinetic coefficient does not only account for a single chemical reaction, but it lumps a number of physical and chemical processes. In Figure 18 $\mathrm{Da_{dev}}$ is represented as a function of temperature for the devolatilization kinetics given for wood in Table 6.

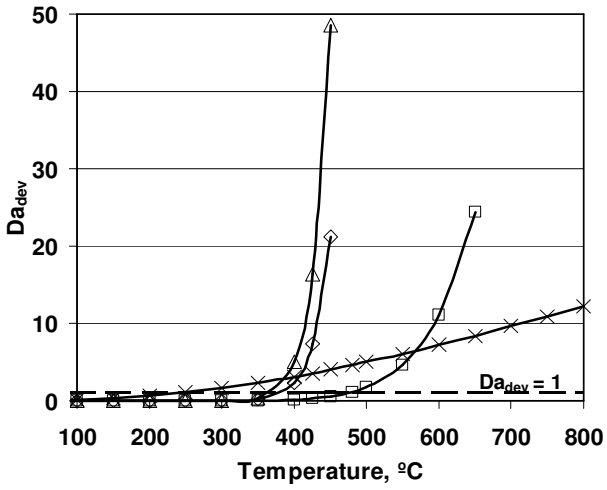

Figure 18: $\mathrm{Da_{dev}}$ as a function of temperature for different devolatilization kinetics from literature: (◊) Davidsson et al. (54), (Δ) Kosstrin (55), (□) Brink (56), (×) Jand and Foscolo (6).

The value of T_{dev} is determined by the intersection of the $\mathrm{Da_{dev}}$–T curve with $\mathrm{Da_{dev}}$= 1. As can be seen the increase of $\mathrm{Da_{dev}}$ with T near T_{dev} is small for the kinetics proposed by Jand and Foscolo[7]. The reason is that Jand and Foscolo's kinetics has low activation energy (see Table 6), because the authors included the effect of particle size into the kinetic equation. The Kosstrin's and Davidsson's kinetics makes $\mathrm{Da_{dev}}$ to be more sensitive to T than Brink's kinetics (higher slopes above T_{dev} in Figure 18), but the use of Brink's kinetics yields to better estimation of T_{dev}, and so, to better prediction of t_{90}.

Experimental results can be employed to evaluate the process limiting the devolatilization rate. This is done by carrying out experiments with different particle sizes and fitting the devolatilization times to an nth order function of particle size:

$$t_{dev} = kd^n \tag{20}$$

being k a parameter whose value depends on the rector temperature. The n value gives information about the mode of conversion. If n=0, t_{dev} does not depend on the particle size, and the devolatilization rate is determined by kinetics. If n=1, the external heat transfer limits the devolatilization rate and if n=2, the process is limited by intraparticle heat transfer. This method has been applied to pyrolysis of DSS[21] and the resulting n value ranged between 1 and 2, which indicates that the both external and internal heat transfer limit the devolatilization rate.

A more realistic way to describe the variations of devolatilization time with particle size is to fit t_{dev} to a quadratic function of d. This is derived by the fact that in many systems, the mode of conversion depends on the particle size; for very small particles the kinetic regime is approached and for large particles the internal heat transfer is limiting and, in addition, there may exist an intermediate range of particle sizes for which the external heat transfer is limiting.

In this work, t_{60} for DSS was fitted to a quadratic function of the particle size:

$$t_{60} = b_0 + b_1 \cdot d_p + b_2 \cdot d_p^{\,2} \tag{21}$$

The values of the parameters b_o, b_1 and b_2 depend on the bed temperature according to the following expressions:

$$b_0 = 15.682 - 0.0004 T_b \tag{22}$$

$$b_1 = 16.943 - 0.0192 T_b \tag{23}$$

$$b_2 = -1.737 + 0.0027 T_b \tag{24}$$

T_b is expressed in ºC, d_p is in mm and and t_{60} in s.

The model described by eqs (3)-(10) was employed to simulate the conversion of wood pellets and DSS granulates.

5.3 Wood pellet simulation

Wood pellet was assumed to be an infinite cylinder, in order to apply the model developed. This assumption has been shown to yield good results under FB combustion conditions as long as the length to diameter ratio is larger than 3[48]. The validity of this simplification was verified by observing no difference in the conversion curves obtained from tests carried out with 1 pellet of 25 mm and two pellets of 12.5 mm length.

Figure 9 shows the temperatures at the surface and centre of a wood pellet, calculated using the model and the conversion determined experimentally (see eq 1) for a bed temperature of 800ºC. The large differences between the two temperature curves indicate that intraparticle temperature gradients are important during devolatilization of wood pellets. In addition, it is observed that conversion is almost complete (>95%) when the particle centre is still below the bed temperature (<750ºC). This indicates that heating up of the particle greatly influences the devolatilization process, in agreement with the Bi and Da_{dev} values in Table 8.

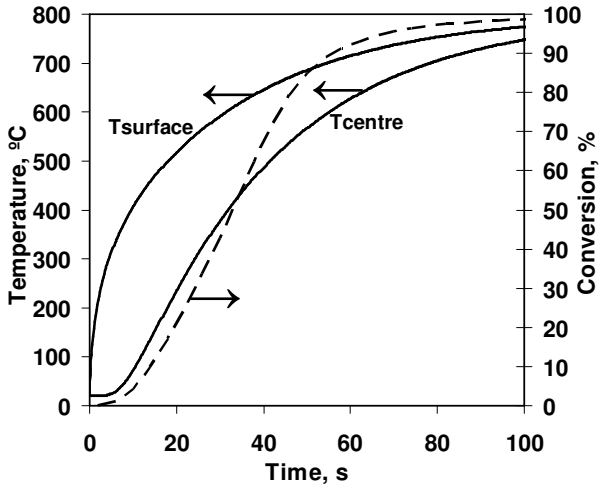

Figure 9: Temperatures at the surface and centre of wood pellets calculated with the model (h=160 W/(m^2 K)) and experimental conversion. (Bed temperature 800ºC).

For simulating the evolution of conversion during the devolatilization of wood pellets the apparent kinetics determined by Jand et al.[7] (see Table 6) was used because it was obtained in very similar setup and operating conditions. A comparison between the results of the simulation and the conversion versus time curves obtained experimentally is shown Figure 10. The model reproduces the conversion of wood pellets fairly well during the whole range of conversion for all temperatures.

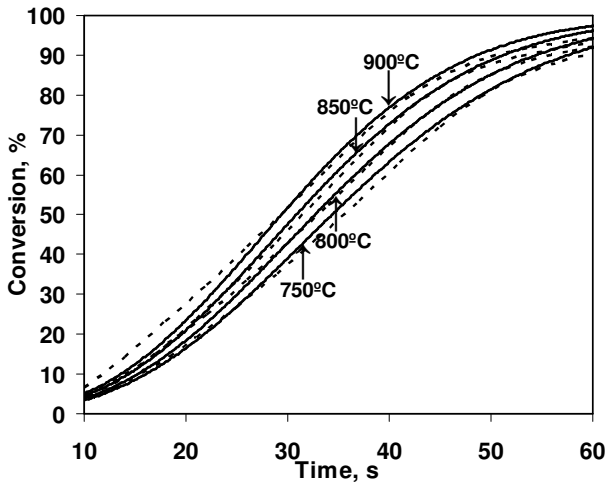

Figure 10: Comparison between simulated (solid lines) and experimental (dashed lines) conversion curves for devolatilization of wood pellets at four bed temperatures.

A sensitivity study was carried out varying the values of the parameters that were assumed to have the most important effect on the conversion times and whose determination can be assumed to be less certain: h, λ_{eff}, E_{dev}, and A_{dev}. The effects of variations in c_p and ρ during devolatilization were assumed to be low, because their values in literature vary less than those of other parameters.

For the sensitivity study the values of the parameters were varied within a range of values found in literature. The low value used for λ_{eff} was taken from[7] and the high value for λ_{eff} was calculated for a 1300 kg/m^3 wood pellet according to[46]. The effect of the kinetic parameters was studied by varying ±50% the E_{dev} and A_{dev} values from[7]. The effect of applying other kinetics was also studied: parameters given by Brink et al.[55], Davidsson et al.[56] and Kosstrin[57] (see Table 6) instead of those given by[7] were used. The high and low values of the different parameters used in the sensitivity study are presented in Table 9 and the results of the analysis are shown in Figure 11.

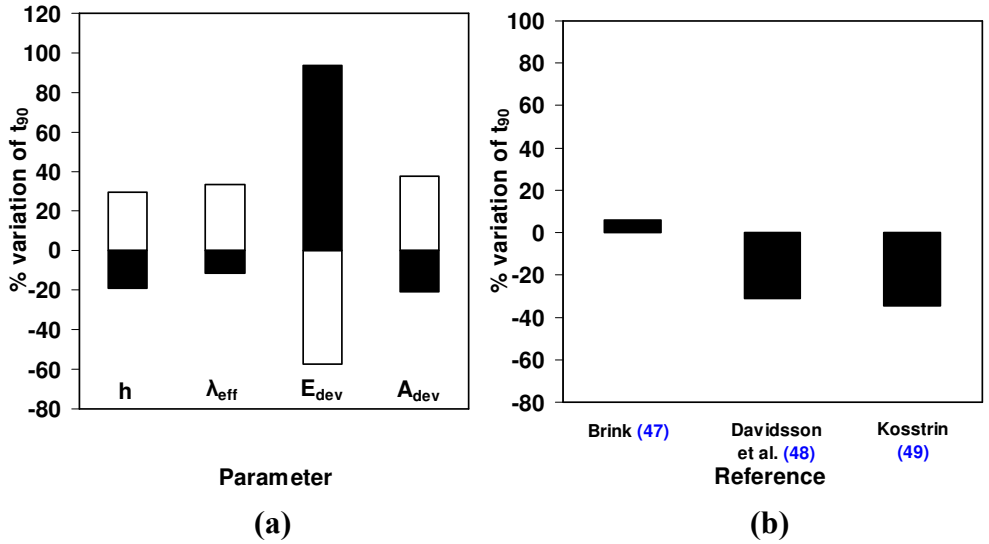

Figure 11: Percentage variation of t_{90} calculated from the model (a) when varying the parameters introduced at the bottom, between the low and high values given in Table 8 and (b) when employing kinetic parameters given by different authors shown in Table 5, (□) % variation with the low parameter value, (■) % variation with the high parameter value.

The results in Figure 11(a) show that both internal and external heat transfer are important, which is consistent with Figure 9. Figures 11(a) and 11(b) also indicate that the choice of kinetic parameters is important. The fact that E_{dev} is the most important parameter in Figure 11(a) does not necessarily imply that the process is controlled by devolatilization kinetics. The choice of kinetic parameters will determine the temperature above which the devolatilization can be considered to be fast, so even if the process is controlled by particle heat up, the kinetic parameters will have a great influence on the devolatilization time. This is further discussed in Appendix 1.

5.4 DSS simulation

The conclusion derived from the scaling analysis, i.e. very rapid pyrolysis kinetics of the DSS, was confirmed to be false. The reason was thought to be that the DSS investigated in this work differs significantly from other DSS. The composition of both the organic and inorganic fractions of the sewage sludge can vary significantly between different sludges depending on the source and treatment process[23]. DSS contains a large amount of different components compared to wood and other biomass, including inorganic substances[58,59]. The addition of different metals and additives during the

sewage plant operation can alter significantly the composition of the sludge generated and then the devolatilization kinetics of the DSS. Therefore, a series of experiments were conducted to obtain the DSS kinetics.

To elucidate the effect of particle size on DSS devolatilization, the model was used to simulate the temperature profiles of DSS granulates with the largest and finest sizes of the DSS received (1.2 and 4.5 mm). Figure 12 was drawn to analyze this effect. Each graph of Figure 11 includes the evolution with time of the experimental conversion as well as the simulated temperature at both, particle surface and in centre. Figure 12(a) corresponds to DSS particles of 1.2 mm, whereas Figure 12(b) stands for DSS particles of 4.5 mm. The simulated temperatures were calculated using h = 250 W/(m^2 K) and h = 185 W/(m^2 K) for 1.2 mm particles and 4.5 mm particles respectively.

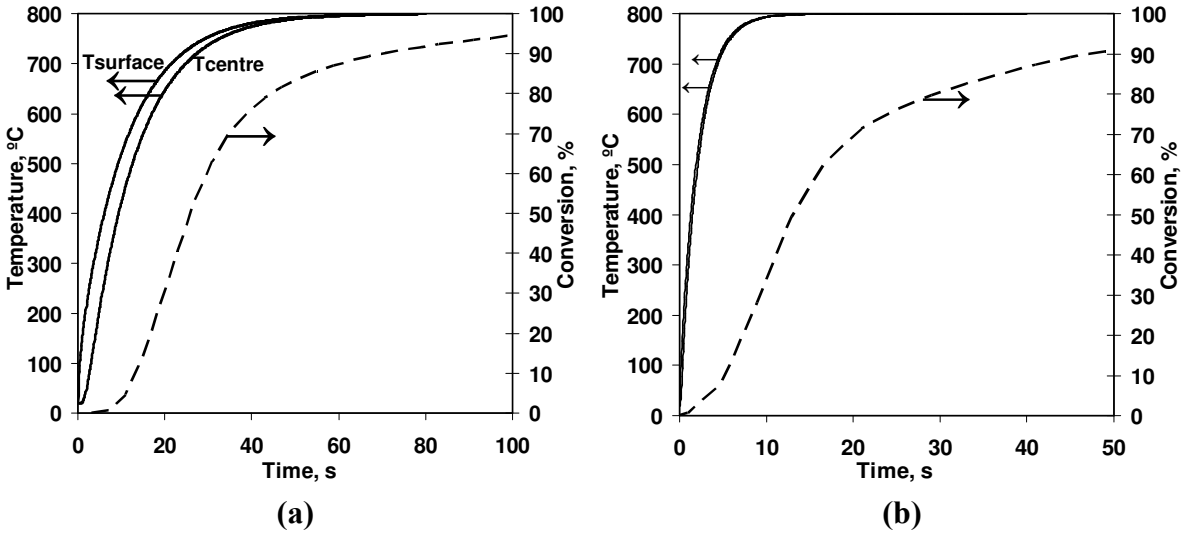

Figure 12: Simulated temperatures at the surface and the centre of the DSS particles (solid lines) and experimental conversion (dashed lines) at T_b=800ºC and u=0.8 m/s. (a) 1.2 mm DSS particles, (b) 4.5 mm DSS particles.

Figure 12(a) shows that 1.2 mm DSS granulates are heated up so quickly that the conversion is limited as the particle has reached the bed temperature. The temperature at the centre of the particle is 790 ºC when the conversion is 10 %. It is observed in Figure 12(a) that the temperatures at the particle centre and at particle surface are very similar during the whole conversion process, so that intraparticle temperature gradients are small.

Figure 12(b) shows that for 4.5 mm DSS particles, intraparticle temperature gradients are small, but more significant than for 1.2 mm particles: the difference between temperatures at the surface and centre of the particle are 89ºC, 74ºC, 52ºC and 31ºC when the conversion is 5%, 10%, 20% and 40% respectively. However, from approximately x_{dev} = 0.60, the temperature gradients vanish. It is observed that the conversion of 4.5 mm particles proceeds slower than for 1.2 mm particles and that the volatiles release overlaps with particle heat up. Figure 13 shows the conversion of 4.5 mm DSS particles at two different fluidizing velocities. The conversion is slower for the lower gas velocity, indicating that the conversion rate is strongly influenced by external heat transfer.

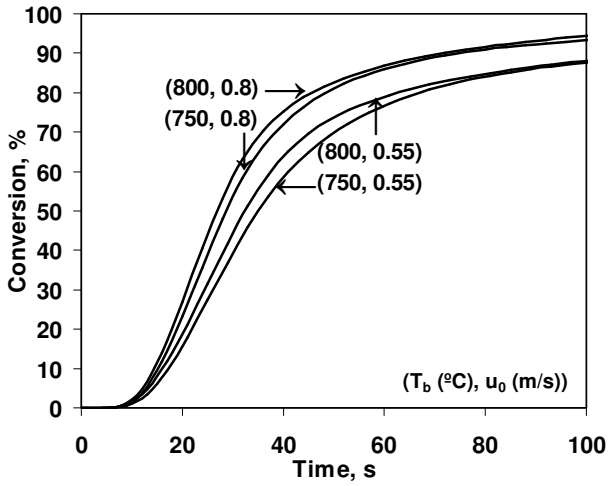

Figure 13: Conversion versus time curves for 4.5 mm DSS particles for two bed temperatures, T_b, 750ºC and 800ºC and two different fluidizing velocities, u, 0.55 m/s and 0.8 m/s.

Drawing the attention again to Figure 12(a), it is observed that from around x_c=0.15, the pyrolysis kinetics can be considered to control the conversion of 1.2 mm DSS particles. Since the temperature gradients inside the particle are small, X_{dev} can be considered to be the same throughout the particle volume and equal to x_{dev} . In addition, given that the conversion is still limited when the particle has reached the bed temperature, the pyrolysis kinetic coefficient k_{dev} at the bed temperature can be approximately obtained by integrating expression in eq (9):

$$k_{dev}(T_b) = \frac{1}{t_{x_{dev}}} \ln\left(\frac{1}{1-x_{dev}}\right) \tag{25}$$

For bed temperatures lower than 800ºC (Figure 12(a) corresponds to devolatilization at 800ºC) the kinetic regime will be reached at even lower conversions. Figure 14 shows t_{xdev} versus ln(1/(1-x_{dev})) for experiments carried out with 1.2 mm DSS particles at 750ºC and 800ºC. The points in Figure 14 are apparently arranged into two lines, suggesting that k_{dev} for conversions below and above 0.70 are different. This means that there are two different dominating processes during DSS thermal conversion. DSS may contain a number of different material fractions with different devolatilization kinetics. As a consequence, the composition of the unconverted material could change during the conversion, leading to a modification of the global devolatilization kinetics. Another possible explanation for the change in kinetic behavior at high conversions is the partial sintering of some material, obstructing the flow of volatiles outwards. This is supported by the fact that the conversion rate is not affected by the bed temperature for conversions above 80% for 4.5 mm particles (see Figure 13).

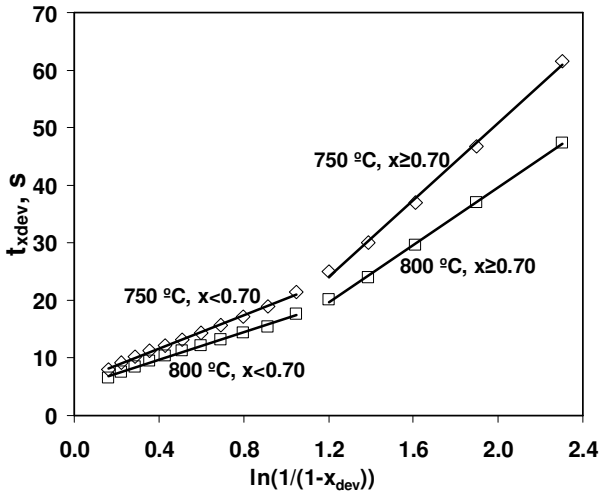

Figure 14: Time of devolatilization to reach conversion x_{dev}, t_{xdev} as a function of ln(1/(1-x_{dev})) for tests conducted with 1.2 mm DSS particles and bed temperatures between 750ºC and 800ºC.

The A_{dev} and E_{dev} for x<0.7 and x≥0.7 obtained from Figure 14 are shown in Table 10. These values vary largely compared to those from[¡Error! No se encuentra el origen de la referencia.] given in Table 7 that were used for the scaling analysis in Table 8(a). It is concluded that the devolatilization kinetics of the DSS tested in this work is much slower than for the DSS tested by Scott et al.[¡Error! No se encuentra el origen de la referencia.]. Using the kinetic parameters in Table 10 at 800ºC, the values of the ratio Da_{dev}/Bi are 0.25-0.61 and 1.20-5.86, for DSS particles of 1.2 mm and 4.5 mm respectively. These values are consistent with the observations made in Figure 11, indicating kinetic control for the small particles, while for the 4.5 mm particles the Da_{dev}/Bi values indicate that mainly particle heat up is important, although the devolatilization kinetics also influences the devolatilization rate.

Conversion range	E_{dev} (J/kmol)	A_{dev} (1/s)
0.15≤x<0.7	$3.63 \cdot 10^7$	4.95
0.7≤x≤0.9	$5.35 \cdot 10^7$	16.15

Table 10: Values for the pre-exponential factor (A_{dev}) and activation energy (E_{dev}) obtained by applying eq (25) to experimental results obtained at 750 ºC and 800 ºC for 1.2 mm DSS particles

The model was developed using the kinetics obtained (Table 10) to simulate the conversion of 4.5 mm DSS particles. The *h* value employed was 185 W/(m^2 K), which is between the values given by eqs (11) and (12). Figure 15 shows the results of the simulation and the experimental results for bed temperatures 750 ºC and 800 ºC. The simulated conversion against time curve agrees well with the experimental curves.

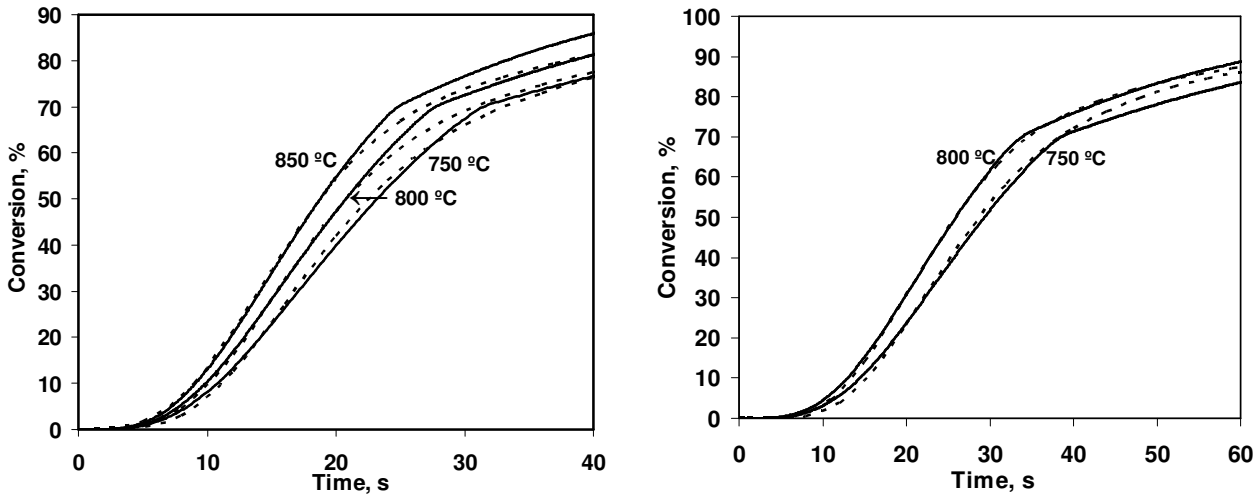

(a) **(b)**

Figure 15: Conversion of DSS particles calculated from the model (solid lines) and conversions obtained experimentally (dashed lines). (a) DSS as received (3.3 mm mean size), (b) 4.5 mm particles.

According to the model presented here, the temperatures at which devolatilization of DSS occurs depend to a large extent on the particle heating rate, which depends on the particle size and bed temperature. This could explain the different product yields obtained at different bed temperatures and with different particle sizes, especially the higher char yields obtained with larger particles. However, the model only gives a qualitative judgment of the plausible reasons but is not capable to quantitatively explain the variation in the observed yields. Moreover, the bed temperature also affects the extent of extraparticle secondary reactions such as thermal cracking of tar and the particle size may influence the extent of intraparticle volatiles reactions. A more rigorous model should be formulated to simulate these effects.

6. CONCLUSIONS

The devolatilization behavior of various biofuels (wood, meat and bone meal, and compost pellets, as well as dried sewage sludge granulates, DSS) was studied in a lab-scale FB between 750 and 900ºC. The yields of char, condensate and light gas, the gas composition, as well as the time of conversion during devolatilization were determined for the different fuels. The yields and gas composition for all the fuels were correlated with bed temperature (eq (2)). The data can be useful for fluidized bed applications involving these fuels. It was fund that both product yields, gas composition and devolatilization times differ significantly between different fuels.

A simple model was developed to understand the mode of conversion of DSS and wood pellets. The other fuels could not be analyzed because of lack of data on fuel properties. The model can be applied to other fluidized bed units if only the proper value for the external heat transfer coefficient, *h,* is applied. The heat up of DSS particles was found to be mainly influenced by external heat transfer, while for wood pellets both internal and external heat transfer were important. The devolatilization of fine DSS particles was found to be controlled by pyrolysis kinetics during most of the conversion period, so the Arrhenius parameters for first-order devolatilization kinetics were determined, given in Table 10. The kinetic parameters were successfully applied to simulate the conversion of large DSS particles. The conversion these particles were found to be influenced by

both particle heat up and kinetics. The kinetic parameters in Table 10 were successfully applied to simulate the conversion of large DSS particles.

A simple model to predict devolatilization time, when the devolatilization kinetics is much faster than the particle heat up, was presented. This model was employed to estimate the devolatilization time for wood pellets applying kinetic parameters from literature. There were great variations between the kinetic parameters presented by different authors and the calculated devolatilization times were found to vary significantly depending on the kinetics employed.

6.1 Future work

In this section, future work to be done within the *FletGas* project is presented. Special emphasis is give to the tasks of the PhD thesis, where this master thesis is included.

In the near future, further DSS devolatilization experiments will be carried out. During the tests not only the light gas and char yields will be determined, but also water and tar will be measured. The composition of the produced tar will be determined and thus not only the global mass balance, but also the carbon, hydrogen and oxygen balances will be checked. At the moment, experiments for the determination of DSS char reactivity with CO_2 are being carried out and when these are completed steam gasification experiments will be done. The acquired devolatilization and char gasification data will be added to a gasifier model that has been developed in Aspen Plus. The model will enable calculation of the reactor temperature, the amount of gas produced and its composition and the achieved char conversion, for different feed rates of fuel, air and steam. These data will be the input for the preliminary design of the pilot plant.

Another task that needs to be completed is the development of a model for the simulation of a fixed bed of char that will support the design of the *chemical quench.* This will be done during a two month period in the *Chalmers University of Technology*, Göteborg, Sweden. The first step is to develop a char particle model to be introduced into a fixed bed model. This model will be employed to simulate the operation of the *chemical quench* under different operating conditions; temperature, flow rate and composition of the inlet gas, char particle size, etc.

For the design of the three stage gasification system, a fluid dynamic model needs to be obtained. For this purpose, experiments will be carried out in a cold model, made up of three fluidized beds and a fixed bed, connected to each other. The complete setup is constructed from transparent plastic.

In this project, a great deal of work will be dedicated to the conversion of tars and both tar formation during devolatilization and secondary reactions will be studied. During dedicated pyrolysis experiments, the influence of heating rate and particle size on the quantity and composition of tar will be determined. The acquired data will be employed to develop a particle devolatilization model that will enable predictions o results obtained under different operating conditions. The activity of secondary tar reactions will be measured in dedicated experiments varying the temperature and composition of the carrier gas. The data acquired during pyrolysis, secondary tar conversion and char

reactivity experiments will be employed to develop a detailed fluidized bed gasification model.

The fluidized bed and *chemical quench* models will enable the whole system to be simulated and the obtained results together with results from pilot plant experiments will be used to optimize the design and operation of a three stage gasification system at industrial scale.

APPENDIX: PROCEDURE FOR CALCULATION OF FUEL PARTICLE TEMPERATURE PROFILES AND CONVERSION AT DIFFERENT TIMES

The temperature field within the particle at different times was solved integrating eqs 3–6 numerically using an explicit scheme. The step size in the radial direction, Δr, was between 0.024 and 0.038 mm. The maximum time step required for the model to converge is given by the following equation:

$$\Delta t \leq \frac{1}{2}\frac{\Delta x^2}{k} \tag{26}$$

The time step employed here was between 0.001 and 0.002 s. The temperature at a certain distance, r, from the particle centre at a certain time, t, T_r^t, was calculated from employing the following expression:

$$T_r^t = \frac{\lambda_{\text{eff}}\Delta t}{\rho c_p}\frac{T_{r+\Delta r}^{t-\Delta t} - 2T_r^{t-\Delta t} + T_{r-\Delta r}^{t-\Delta t}}{\Delta r^2} + \frac{b}{2r\Delta r}(T_{r+\Delta r}^{t-\Delta t} - T_{r-\Delta r}^{t-\Delta t}) \tag{27}$$

Equation (27) enables T^t_r to be calculated from the temperatures at the adjacent sites at time t-Δt.

The temperature at the particle centre is calculated considering eq (6):

$$T_0^t = T_0^{t-\Delta t} + \frac{2\lambda_{\text{eff}}\Delta t}{\rho c_p}\frac{T_{\Delta r}^{t-\Delta t} - T_0^{t-\Delta t}}{\Delta r^2} \tag{28}$$

And the temperature at the particle surface is calculated considering the surface boundary condition (eq (5)):

$$T_R^t = T_R^{t-\Delta t} + \frac{a\Delta t}{\rho c_p \Delta r} \tag{29}$$

$$a = h(T_\infty - T_R^{t-\Delta t}) - \frac{\lambda_{\text{eff}}}{\Delta r}(T_R^{t-\Delta t} - T_{R-\Delta r}^{t-\Delta t}) \tag{30}$$

Equations (27)-(30) enable the temperature fields at a certain time, t, to be calculated once the temperature field at t-Δt is known. At time $t=0$, the temperature throughout the particle is considered to be 20 ºC.
Once the temperature fields have been calculated, the local conversion at each radial position at time t, X_r^t can be calculated:

$$X_r^t = X_r^{t-\Delta t} + k_{\text{dev}}(1 - X_r^{t-\Delta t})\Delta t \tag{31}$$

$$k_{\text{dev}} = A_{\text{dev}} \exp\left(-\frac{E_{\text{dev}}}{R_g T_r^{t-\Delta t}}\right) \tag{32}$$

The particle conversion at time t, x_t can be calculated as follows:

$$x_t = \sum_{r=0}^{R} X_r^t (b+1)\Delta r \frac{r^b}{R^{b+1}} \tag{33}$$

7. NOMENCLATURE

A	pre-exponential factor, s^{-1}
a_0, a_1, a_2	coefficients of Eq. (2)
Ar_i	Archimedes number of inert particle (i), $g d_i^3 \rho_g (\rho_p-\rho_g)/\mu_g^2$
b	geometry factor
Bi	Biot number, hR/λ_{eff}
c_p	specific heat capacity, J/(kg K)
d	particle diameter, m
Da_{dev}	Dahmköhler number, $k_{dev}\rho_p cp_p R^2/\lambda_{eff}$
E	activation energy, J/kmol
h	heat transfer coefficient, W m^{-2}
k	kinetic constant, s^{-1}
Nu_i	Nusselt number for inert particle, hd_i/λ_g,
Nu_p	Nusselt number for active particle, hd_p/λ_g,
Pr	Prandtl number, $cp_g \mu_g/\lambda_g$
R	radius of a sphere/cylinder or the half thickness of a flat particle, m
R_g	universal gas constant, J/(K mol)
r	radial position within a fuel particle, m
S	surface, m^2
T	temperature, K
t	time, s
t_{90}	time for 90% conversion, s
t_{60}	time for 60% conversion, s
u	fluidizing velocity

V	volume, m^3
X	degree of conversion
x	particle conversion

Greek symbols

Θ	dimensionless temperature
λ_{eff}	thermal conductivity, W/(m K)
μ	viscosity, Pa s
$\mu_{1,2}$	coefficients of eq (14)
ρ	density, kg/m^3
τ	characteristic time for particle heat up, s
Ψ	particle sphericity

Subscripts

dev	devolatilization
eh	external heat transfer
eq	equivalent
g	gas
i	inert particles
ih	internal heat transfer
p	particle
0	at time = 0
∞	at time = ∞
ref	reference

Abbreviations

daf	dry and ash free
DSS	dried sewage sludge
FB	fluidized bed
ID	inner diameter
MBM	meat and bone meal
wt%	percentage on weight basis

8. REFERENCES

(1) Devi, L.; Ptasinski, K.J.; Janssen, F.J.J.G. *Biomass and Bioenergy*, **2002**, 24,125-140.

(2) Campoy, M.; Gómez-Barea, A.; Nilsson, S.; Fuentes-Cano, D.; Ollero, P. *Proceedings of 17th European Biomass Conference & Exhibition.* Hamburg, Germany, 2009**.**

(3) Kersten, S.R.A.; Wang, X.; Prins, W.; Van Swaaij, W.P.M. *Ind. Eng. Chem. Res.* **2005,** 44, 8773-8785.

(4) Raveendran, K.; Ganesh, A.; Khilar, K.C. *Fuel* **1996,** 75, 987-998.

(5) Rao, T.R.; Sharma, *Energy*, **1998**, 23, 973-978.

(6) van den Aarsen, F. G. *Ph.D. Dissertation*; Twente University Publication: University of Twente, 1985.

(7) Jand, N.; Foscolo, P.U. *Ind. Eng. Chem. Res.* **2005**, 44, 5079–89.

(8) Nunn, T.R.; Howard, J.B.; Longwell, J.P.; Peters, W.A. *Ind. Eng. Chem. Process Des. Dev.* **1985**, 24, 836-844.

(9) Thunman, H.; Niklasson, F.; Johnsson, F.; Leckner, B. *Energy & Fuels* **2001**, 15, 1488–1497.

(10) Di Blasi, C.; Branca, C.; Santoro, A.; Hernandez, E.A. *Combustion and flame*, **2001**, 124, 165-177.

(11) Mohan, D.; Pittman, C.U.; Steele, P.H. *Energy and Fuels*, **2006,** 20, 848-889.

(12) Di Blasi, C. *Progres in Energy and Combustion Science*, **2008**, 35, 121-140

(13) Boronson, M.L; Howard, J.B; Longwell, J.P; Peters, A.W. *AIChE J*, **1989**, 35, 120-128.

(14) Scott, D.S; Piskorz, J. *Can. J. Chem. Eng.*, **1984**, 62, 404-412.

(15) Boronson, M.L.; Howard, J.B.; Longwell, J.P.; Peters, A.W. *AIChE J*, **1989**, 35, 120-128.

(16) Morf, P.; Hasler, P.; Nussbaumer T. *Fuel*, **2002**, 81, 843-853.

(17) Hajaligol, M.R.; Howard, J.B.; Longwell, J.P.; Peters, W.A. *Ind. Eng. Chem. Process Des. Dev.* **1982**, 21, 457-465.

(18) Rath, J.; Steiner, G.; Wolfinger, M.G.; Staudinger, G. *J. Anal. Appl. Pyrol.* **2002**, 62, 83-92.
(19) Roberts, A.F. *Combustion and Flame* **1970**, 14, 261–272.

(20) McDonnell, K.; Desmond, J.; Leahy, J.J.; Howard-Hildige, R.; Ward, S. *Energy* **2001**, 26, 81-90.

(21) Scott, S.A.; Davidson, J.F.; Dennis, J.S.; Hayhurst, A.N. *Chemical Engineering Science* **2007,** 62, 584-598.

(22) Tian, F.-J.; Li, B.-Q.; Chen, Y.; Li, C.-Z. *Fuel* **2002**, 81, 2203-2208.

(23) Fonts, I.; Azuara, M.; Gea, G.; Murillo, M.B. *Journal of Analytical and Applied Pyrolysis*, **2009**, 85, 184-191.

(24) Kaminsky, W.; Kummer, A.B. *Journal of Analytical and Applied Pyrolysis*, **1989**, 16, 27-35.

(25) Inguanzo, M.; Domínguez, A.; Menéndez, J.A.; Blanco, C.G.; Pis, J.J. *Journal of Analytical and Applied Pyrolysis*, **2002**, 63, 209-222.

(26) Bilbao, R.; Millera, A.; Arauzo, J. *Fuel* **1988**, 67, 1586-1588.

(27) Chen, G.; Andries, J.; Luo, Z.; Spliethoff, H. *Energy Conversion and Management,* **2003**, 44, 1875-1884.

(28) Di Blasi, C.; Signorelli, G,; Di Russo, C,; Rea, G. *Ind. and Eng. Chem. Res.* **1999,** 38, 2216-2224.

(29) Fagbemi, L.; Khezami, L.; Capart, R. *Applied Energy* **2001,** 69, 293-306.

(30) Sakoda, A.; Sadakata, M.; Koya, T.; Furusawa, T.; Kunii, D. *The Chemical Engineering Journal*, **1981**, 22, 221-227.

(31) Figueiredo, J.L.; Valenzuela, C.; Bernalte, A.; Encinar, J.M. . *Fuel* **1989**, 68, 1012-1016.

(32) Ayllón, M.; Aznar, M.; Sánchez, J.L.; Gea, G.; Arauzo, J. *Chemical Engineering Journal*, **2006**, 121, 85-96.

(33) Grønli, M.G.; Várhegyi, G.; Di Blasi, C. *Industrial and Engineering Chemistry Research*, **2002,** 41, 4201-4208.

(34) Stengsen, M.; Jensen, A.; Dam-Johansen, K. In Bridgewater, A.V., Blackwell Science:Oxford, UK, 2001;ppm1061-1075.

(35) Wang, X., Kersten, S.R.A., Prins, W., Van Swaaij, W.P.M. *Ind. Eng. Chem. Res.* **2005,** 44, 8786-8795.

(36) Gómez-Barea, A.; Leckner, B. Submitted for publication Sept 2009.

(37) Thunman, H; Leckner B.; Niklasson, F.; Johnsson F. *Comustion and Flame* **2002**, 129, 30–46.

(38) Neves, D.; Thunman, H.; Seemann, M.; Ideias, P.; Matos, A.; Tarelho, L.; Gómez-Barea, A. *Proceedings of 17th European Biomass Conference & Exhibition.* Hamburg, Germany, 2009**.**

(39) Pyle, D.L.; Zaror, C.A. *Chem. Eng. Sci.* **1984**, 39, 147-158.

(40) Chaala, A.; Roy, C. *Environmental Science and Technology* **2003,** 37, 4517-4522.

(41) Di Blasi, C.; Signorelli, G,; Di Russo, C,; Rea, G. *Ind. and Eng. Chem. Res.* **1999,** 38, 2216-2224.

(42) Di Blasi, C.*Chemical Engineering Science* **1996**, 51, 1121-1132.

(43) Zanzi, R.; Sjöström, K.; Björnbom, E. *Biomass and Bioenergy* **2002**, 23, 357-366.

(44) Antal, M. J.; Allen, S. G.; Dai, X.; Shimizu, B.; Tam, M. S.; Grønli, M. G. *Ind. Eng. Chem. Res.* **2000**, 39, 4024 -4031.

(45) Di Blasi, C. *Fuel* **1997**, 76, 957-964.

(46) Antal, Jr. MJ.; Varhegyi, G. Ind. *and Eng. Chem. Res.* **1995**, 34, 703-717.

(47) Rapagnà, S.; Latif, A. *Biomass and Bioenergy* **1997**, 12, 281-288.

(48) Sreekanth, M.; Kolar, A.K.; Leckner, B. *Fuel Processing Technology* **2008,** 89, 838-850.

(49) Gronli, M.G., Melaaen, M.C. *Energy and Fuels* **2000,** 14, 791-800.

(50) Dupont, C.; Boissonnet, G.; Seiler, J.M.; Gauthier, P.; Schweich, D. *Fuel* **2006**, 86, 32–40.

(51) Leckner, B. In: Crowe, C.T. *Multiphase Flow Handbook*; CRC Press, 2006; chapter 5.2.

(52) Palchonok, G. *Ph.D. Dissertation*; Chalmers University of Technology, Gothenburg, Sweden, 1998.

(53) Leckner, B.; Hansson, K.-M.; Tullin, C.; Borodulya, A.V.; Dikalenko, V.I.; Palchonok, G.I. *Proceedings of the 15th International Conference on Fluidized Bed Combustion.* Savannah, Georgia, 1999: Paper 47.

(54) Hartman, M.; Pohořelý, M.; Trnka, O. *Powder Technology* **2007**, 178, 166-172.

(55) Brink, D.L.; Massoudi, M.S. *J Fire Flammability* **1978**, 9, 176-188.

(56) Davidsson, K.O.; Pettersson, J.B.C.; Bellais, M.; Liliedahl, T.; Sjöström, K. in: Bridgwater; A.V., *Progress in thermochemical biomass conversion*, Blackwell Science, 2001; pp. 1129–42.

(57) Kosstrin, H. Proc. Spec. Workshop on fast pyrolysis of biomass, Cooper Mountain, Colorado, USA, 1980; PP. 105-121.